MINISTRY OF EDUCATION AND SCIENCE OF THE REPUBLIC OF KAZAKHSTAN
Non-profit join - stock corporation
ALMATY UNIVERSITY OF POWER ENGINEERING AND TELECOMMUNICATION named after G. Daukeev
Department of *Electronics and robotics*

«Allowed to defense»
The head of department of «Electronics and robotics»
Chigambayev T.O. c.t.s., associate professor
(Full name, academic degree, rank)

____«____» ________________2020 year
(sign)

DEGREE PROJECT

On the topic: *Design and study of knee exoskeleton based on artificial muscles*

Done by: *Amankosov Tilek* *PSa-16-3*
(Surname and initials of a student) (group)

Specialty *5B071600 Instrumentation Engineering*

Research supervisor *Balbayev G.K. PhD, docent*
(Surname, academic degree, rank)

______«____» ________________2020 year
(sign)

Consultants
on economic part: *Tuzelbayev B.I. Ph.D, associate professor*
(Surname, academic degree, rank)

______«____» ________________2020 year
(sign)

on life and environmental safety part: *Begimbetova A.S. Ph.D, senior lecturer*
(Surname, academic degree, rank)

______«____» ________________2020 year
(sign)

Compliance supervisor: *Fazylova A.R.senior lecturer*
(Surname, academic degree, rank)

______«____» ________________2020 year
(sign)

Almaty, 2020

MINISTRY OF EDUCATION AND SCIENCE OF THE REPUBLIC OF KAZAKHSTAN
Non-profit join - stock corporation
ALMATY UNIVERSITY OF POWER ENGINEERING AND TELECOMMUNICATION named after G. Daukeev

Institute of___________*space engineering and telecommunications*______________
Department of_______*Electronics and robotics*________________________________
Specialty___________*5B071600 Instrumentation Engineering*_________________

ASSIGNMENT
for execution of degree project

Student____________*Amankosov Tilek Galiakhmetuli*_________________________
(Full name)

Topic of the work____*Design and study of knee exoskeleton based on artificial muscles*____

Approved by the order of the rector № 155 from « 23 » October 2020 y.

Deadline of the finished work « 8 » June 2020 y.

Initial data required parameters of the results and initial data:

1. *Arduino Mega 2560 microcontroller*
2. *ASUS ROG laptop*

List of issues to be developed in a degree project or a summary:

1. *Artificial muscle analytical review*
2. *Kinematics analysis and optimization of the exoskeleton's knee joint*
3. *Technical part of the work*
4. *Development of life safety measures*
5. *Economic justification of the project*

List of graphical material (with precise indication of mandatory drawings);
This degree project contains 27 figures and tables

Recommended basic literature:

1. *Z. Xiaobiao, "Design of a Control System for a Lower Limb Exoskeleton Rehabilitation Walking Robot", Shanghai Jiao Tong University, China, 2013.*
2. *Villegas, D.; van Damme, M.; Vanderborght, B.; Beyl, P.; Lefeber, D. Third-Generation Pleated Pneumatic Artificial Muscles for Robotic Applications: Development and Comparison with McKibben Muscle. Adv. Robot. 2012, 26, 1205–1227*

Consultants for work with indication of the relevant section

Section	Consultant	Date	Sign
Life safety	*Begimbetova A.S*	*16.05.2020*	
Economic part	*Tuzelbayev B.I*	*18.05.2020*	

SCHEDULE
Of degree project preparation

№	Title of section, list of issues to be developed	Deadline for submission to instructor	Note
1	*Theoretical part*	*29.01*	
2	*Engineering part*	*05.03*	
3	*Program part*	*15.05*	
4	*Life safety*	*16.05*	
5	*Economic part*	*18.05*	
6	*Conclusion*	*06.06*	

Date of issue of the assignment *« 20 » 01 2020 year*

The head of department _________*Chigambayev T.O.*________________________
(sign) (Surname and initials)

Supervisor: ____________________*Fazylova A.R.senior lecturer*______________
(sign) (Surname and initials)

The assignment for execution is accepted by: _________*Amankosov T.G*________
(sign) (Surname and initials)

Аннотация

Объектом исследования является искусственная мышца и экзоскелет колена на основе искусственной мышцы.

Цель работы — создание экзоскелета колена на основе искусственной мышцы.

В результате исследования искусственной мышцы реализован прототип; составлена документация в виде функциональных схем, схем внешних проводок и их подключения; разработаны алгоритмы управления; получена модель системы; разработано программное обеспечение; построены виртуальная 3D модель коленного экзоскелета.

Андатпа

Зерттеу нысаны - жасанды бұлшықет және жасанды бұлшықетке негізделген тізенің экзоскелеті.

Жұмыстың мақсаты - жасанды бұлшықетке негізделген тізенің экзоскелетін құру.

Жасанды бұлшықетті зерттеу нәтижесінде прототип жасалды; Құжаттама функционалды диаграммалар, сыртқы электр сұлбалары және олардың қосылыстары түрінде жасалды; басқару алгоритмдері әзірленді; алынған жүйе моделі; бағдарламалық жасақтама әзірленді; тізе экзоскелетінің 3D виртуалды моделін жасады.

Annotation

The object of study is an artificial muscle and an exoskeleton of a knee based on an artificial muscle.

The purpose of the work is the creation of an exoskeleton of the knee based on artificial muscle.

As a result of the study of artificial muscle, a prototype was implemented; The documentation was compiled in the form of functional diagrams, external wiring diagrams and their connections; developed control algorithms; system model obtained; software developed; built a virtual 3D model of the knee exoskeleton.

Content

Introduction

Today, various devices are widely used: they consist of two main elements: man, and machine. The interaction of these elements determines the quality of the system as a whole. Such devices include substances called exoskeletons (exoskeletons) and are used to enhance human functionality. Separation of exoskeletons for restoration of the musculoskeletal system based on physiotherapy based on measurements carried out using mechanotherapeutic devices. Of particular interest are devices that facilitate movement, heavy weight and significantly increase a person's capabilities, which requires considerable effort for various activities.

There are many rehabilitation systems based on the principle of an external exoskeleton, which allows you to restore the function of individual joints of the lower and upper extremities, but such devices are controlled in software without taking into account the device's interaction with the patient's hands.

More recently, the development of the exoskeleton has allowed complex movements on both sides of the lower and upper extremities. Such devices allow a person to move in space, even if the lower limbs are damaged. In addition, this opens up the possibility of significantly increasing the carrying capacity associated with the performance of tasks, raising the distance to which a person cannot work in normal conditions.

When creating such devices, if there is a theory that developed such systems, special attention should be paid to control issues, taking into account the interaction of man and machine.

In this work, special attention is paid to monitoring the active position of the patient, the controlled movement of the knees and leukopogalas, and also explores a device that allows the patient to move from a sitting position. Methods and tools will be developed for the design of robot electric drives in the modes of lifting the human body and vice versa. A method will also be developed for managing such complex processes of movement, which will help create highly efficient systems that will help people and expand their functional capabilities. The use of such devices significantly increases the effectiveness of rehabilitation measures.

The aim of the study is to develop a theoretical framework and tools for the design of exoskeletons for people with disabilities.

To achieve this goal, it is necessary to solve a number of problems:

1. Fragments of the structure repeat the structure of the upper part of the face.
2. The design should be light and strong at the same time.
3. The exoskeleton should be made of safe materials.
4. It should be possible to change the design of the exoskeleton for the disabled.
5. Regardless of energy sources.
6. In order to survive in the exoskeleton of the lower limb, there must be a certain range of motion for large joints to perform normal motor activity.

1 Artificial muscle analytical review

1.1 Introduction to artificial muscles

Joseph L. McKibben was firstly introduced the McKibben artificial muscle as the most important type of pneumatic artificial muscle (PAMs) in the 1950s to assist paralyzed people.

Pneumatic McKibben muscle was then used as a finger driven flexor hinge splints to provide the pretension force. The Bridgestone rubber company (Japan) commercialized the idea in the 1980s under the name of Rubbertuators. The muscle normally includes an expandable elastic inner tube surrounded by a braided shell. The muscle usually operates with pressurized gas and the system requires a compressor as well as a gas storage container.

The fact is that all this mechanics is not too durable and also has a rather low efficiency. All this is the result of a constant struggle against friction that occurs inside mechanisms. The muscle fibers of living creatures are much more energy efficient, which is why engineers are trying to create an artificial analogue of biological muscles.

The pressurized air is used to increase the volume of the inner bladder and subsequently deform the braided sleeve that make up the McKibben muscle.

The required compressors in the conventional McKibben muscles, however, make the actuation system heavy and bulky and unsuitable to be utilized as microactuators or in portable applications where a compact size and weight minimization are desired. These types of actuators are normally easy to manufacture in a variety of sizes and also commercially available to purchase in the market. The basic working concept of McKibben artificial muscles is that the braided sleeve translates the volumetric increase of the inner bladder to a lengthwise contraction of the braid that is capable of generating contractile forces (figure 1.1) much greater than an equivalent hydraulic or pneumatic system.

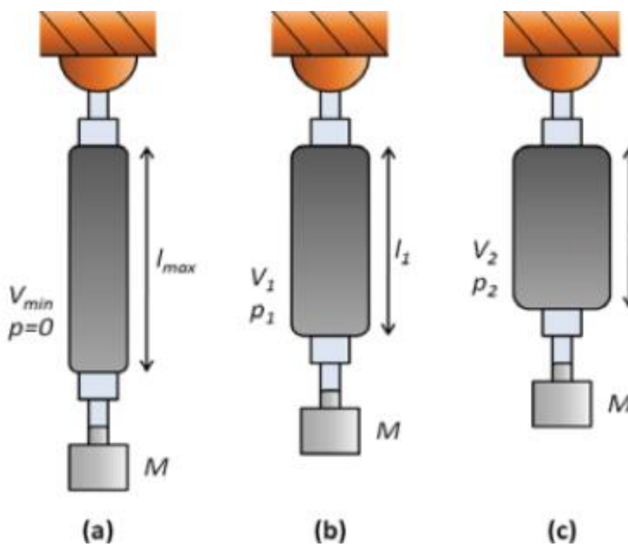

Figure 1.1 - PAM operation under constant load (a) rest state (b) partially inflated (c) fully inflated

It is clear that, when the network shrinks in the length direction, the initial angle moves from α_0 to α and consequently the network maintains it rectangular shape. At the same time a width also increasing from L_0 to L and a length decreasing from l_0 to l and with assuming soft pantograph network in the form of cylinder then initial radius of r_0 and $L = 2\pi r$. Thus, the following equation can be proposed by assuming the side of each pantograph remains constant during the actuation. According to Tondu et al. the ideal McKibben artificial muscle can be assumed as a planar network of jointed identical pantographs as shown in figure 1.2. Where, *m* columns and *n* rows whose envelop is a rectangle of initial length l_0 and width L_0. The initial angle of each elementary pantograph is α_0

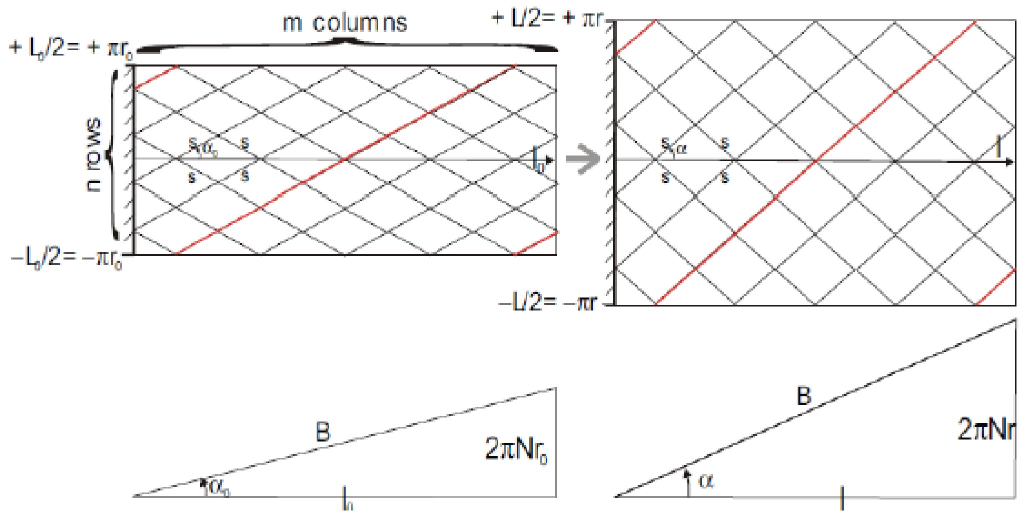

Figure 1.2 - Geometrical characterization of the braided sheath of the McKibben muscle.

$$\frac{r}{r_0} = \frac{\sin \propto}{\sin \propto_0} \tag{1.1}$$

Subsequently the contraction function is:

$$f(\varepsilon) = \frac{1}{\sin \propto_0}\sqrt{1 - \cos \propto_0{}^2\,(1-\varepsilon)^2} \tag{1.2}$$

And by applying the general muscle force equation to the proposed contraction function
above, we can conclude that the tensile force generated by the ideal PAM ($F_{idealcyl}$) depends
upon the contraction strain ($\varepsilon = \Delta l/lo$) as (P= Internal pressure):

$$F_{idealcyl}(\varepsilon) = (\pi r_0^2)P\,[a(1-\varepsilon)^2\ - b], \qquad 0 \le \varepsilon \le \varepsilon_{max} \tag{1.3}$$

$$a = \frac{3}{\tan {\propto_0}^2} \quad and \quad b = \frac{1}{\sin {\propto_0}^2} \tag{1.4}$$

As a result, the muscle normally produces the maximum force when the contraction strain (ε) is zero as below:

$$F_{ideal\,cyl\,max} = (\pi r_0^2)P(a-b) \tag{1.5}$$

Based on above simple equation, generated force is a function of initial angle of the braided sleeve, internal pressure and muscle radius. It appears that, the generated force decreases significantly with increasing the initial angle up to critical angle which is 54.44º and then the muscle produces negative forces which can be interpreted as an expansion instead of contraction. It was found that the muscle generates higher forces for the same initial angle and radius with increasing the amount of internal pressure. The difference between red and black lines is more significant in the lower initial angles. Figure 1.3 shows the dependency of the generated force on initial angle and internal pressure.

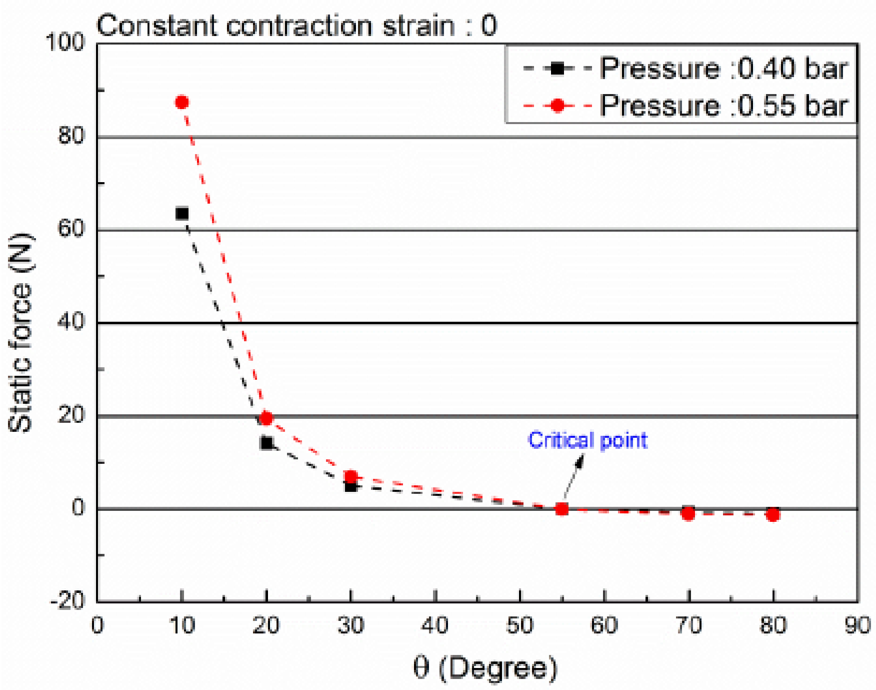

Figure 1.3. The relationship between maximum generated force and initial angle of the braid for PAMs with a starting radius of 1 mm and pressurized to either 0.40 or 0.55 bar.

It is also important to note that according to the equation 1.6 the muscle generates the highest contraction strain when the generated force is 0:

$$\varepsilon_{ideal\,cyl\,max} = 1 - \left(\frac{1}{1.732\ \cos\alpha}\right) \tag{1.6}$$

Equation 1.6 indicates that the amount of contraction strain of the muscle only depends on initial angle of the braided sleeve and is independent of internal pressure. The amount of contraction strain reduces with increasing the initial angle (similar to the force trend in equation 1.6) and reaching zero contraction strain at critical angle (54.44º). The behavior of the muscle changes dramatically above the critical angle and produces expansion strains, the phenomena that also were observed in force behavior (equation 1.6). This behavior proves that McKibben artificial muscles can be adjusted for specific applications where either expansion or contraction strains are required. Figure 1.4 shows the dependency of contraction strain on initial angle of the braided sleeve.

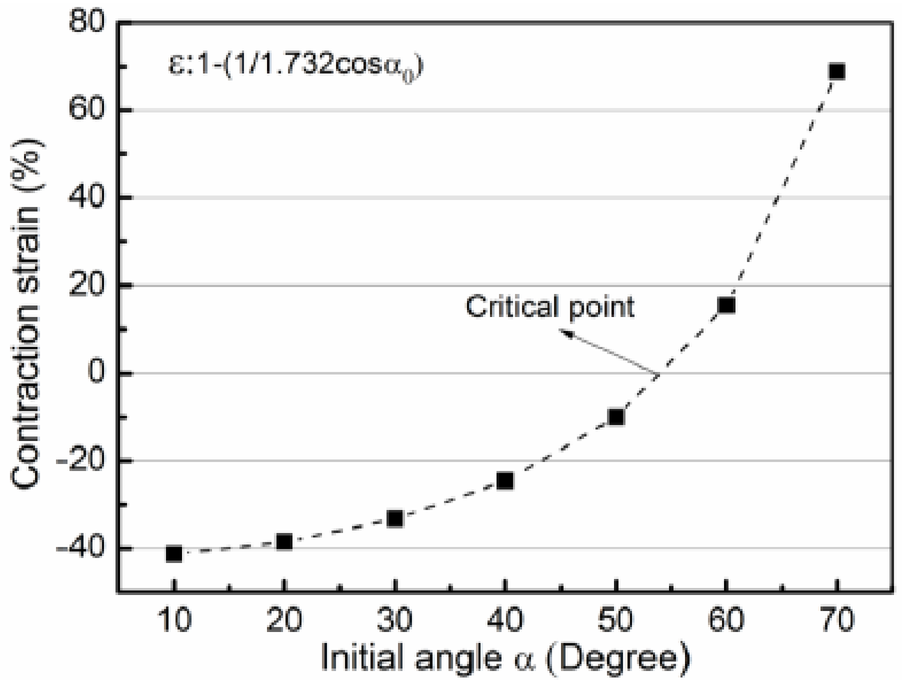

Figure 1.4. The relationship between contraction strain and initial angle of the braid.

This particular artificial muscle, however, presents some disadvantages such as the requirement of a separated mechanical air compressor, a noisy system, a heavy system to carry for human or robots and high electricity consumption. To overcome mentioned disadvantages several attempts, have recently been made to replace the air with water or chemo-sensitive materials to introduce more compact and less noisy system.

1.2 The effect of braided sleeve structure on performance of novel conductive and bladderless paraffin filled McKibben muscle

To arrange of the utilize of bladder inside the unused bladderless, paraffin filled McKibben muscle, two basic concepts have been considered which are particularly related to the braid structure. Authentic braid examination and arrange is required to viably dodge the paraffin spilling from the conductive braid in fact over the wax dissolving temperature. The sensibility of containing fluid paraffin interior a braid can be surveyed utilizing the approach utilized for penetrable layers. The weight required to thrust a non-wetting fluid through the pores of a layer is called the breakthrough weight, P, and is related to the film and fluid properties by the taking after Young–Laplace condition:

$$P = -\frac{2\sigma \cos\theta}{r} \quad (1.7)$$

Where, r, is span of the pores, σ and Θ are the surface pressure of the fluid and the contact point, separately. For any match of materials, the breakthrough weight increments as the measure of pores diminishes.

According to equation 1.8 the cover factor is a function of braid diameter, db, initial braid angle, $\frac{\alpha}{2}$, yarn width, wy and number of threads, Nc. In this research, the cover factor of the braided sleeve was varied and assessed in terms of its ability to prevent the paraffin wax exuding from the braided sleeve in the expanded state.

The fact is that all this mechanics is not too durable and also has a rather low efficiency. All this is the result of a constant struggle against friction that occurs inside mechanisms. The muscle fibers of living creatures are much more energy efficient, which is why engineers are trying to create an artificial analogue of biological muscles.

The cover figure was shifted by autonomously diminishing the distance across of the braid as well as expanding the yarn width. Pore sizes in a braid can be communicated in terms of the cover figure, C, which is characterized as the proportion of the zone possessed by the yarn inside an occasional pore unit to the entire region of the pore unit, as appeared in figure 1.5.

$$C = \frac{W_y N_c}{\pi d_b \cos\frac{\alpha}{2}} - \left[\frac{W_y N_c}{2\pi d_b \cos\frac{\alpha}{2}}\right]^2 \quad (1.8)$$

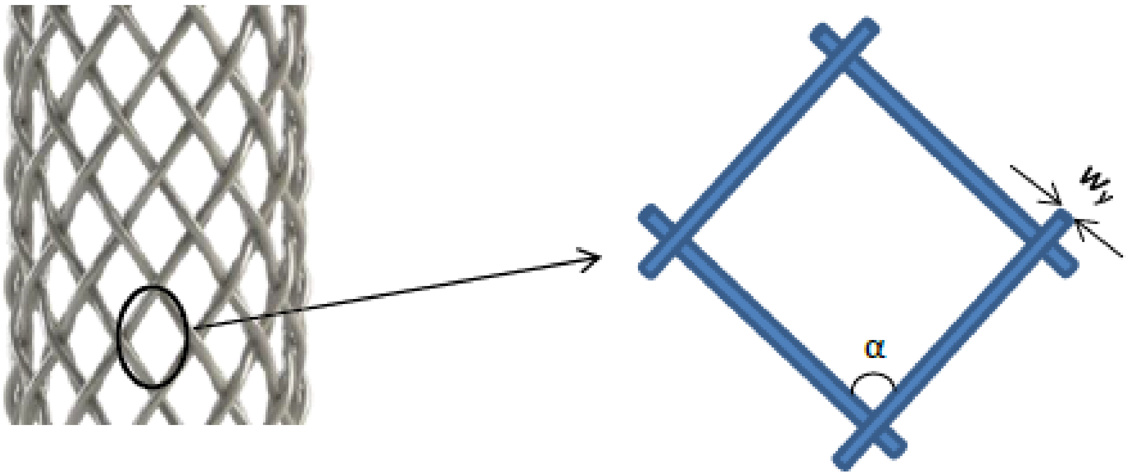

Figure 1.5. The schematic view of conductive braided sleeve indicating the diamond shaped periodic pore unit.

1.3 Actuation Testing of the McKibben Muscle Using the Braided Sleeve

The muscle built utilizing the bladder made with dis-connected crossing points may be pressurized to 0.66 bar without disillusionment. Loosening up of the made oblige happened completely on depressurization. These comes almost were dependably observed in the midst of four successive pressurization depressurization cycles. This muscle offers thrust of 0.053 MPa (960 mN) which is 2.2 times less than HAM muscle displayed in Chapter. 1 with comparable length and implanted weight (35 mm and 0.66 bar) but different starting braid point ($\alpha0=30$ and $\alpha0=35$). The performance of this muscle is additionally essentially less than anticipated information (F= 5.96 N, Compression= 33.3%). It is most likely since of the diverse structure of the braided sleeve utilized in this Chapter. In this Chapter non-woven type of structure was used instead of woven structure which is common in conventional braided sleeves. Woven structure normally defines as a structure which the fibers are decussately on top and bottom of each other. In non-woven structure therefore, the fibers are either on top or bottom of each other. Taking to account the diameter and length of this muscle, the generated isometric force is also reasonable in comparison to previous HAMs systems. Figure 1.6 appears that a most extraordinary isometric obliges of 960 mN was recorded for the 35 mm long muscle in reasonable 1.3 s.

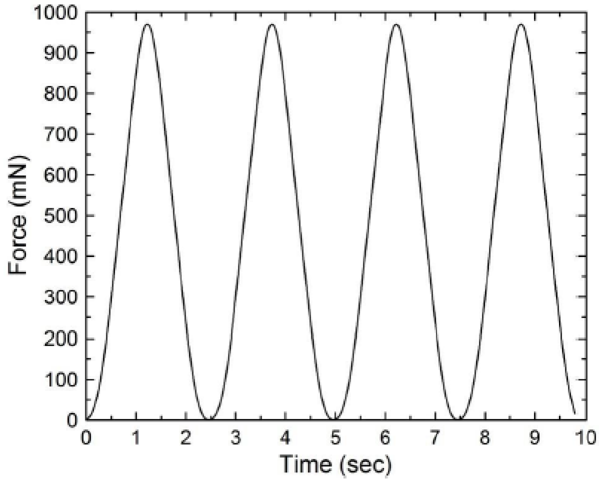

Figure 1.6. Isometric force tests under constant air pressure (0.66 bar). Pressurization-depressurization test was performed four different cycles.

An isotonic test was besides performed underneath a stack of 12 mN and talk about weight of 0.66 bar associated for 1 s and after that released. The strain totally recovered in the midst of depressurization and the muscle showed up uncommonly dependable behavior in the midst of four pressurizing / depressurizing cycles. Comparable to the push produced, the withdrawal strain created with this muscle is 1.7 times less than HAM muscle presented in Chapter. 2 with comparable length and infused weight (35 mm and 0.66 bar) but diverse introductory braid point (α_0=30 and α_0=35). Figure. 1.7 appears that the muscle contracted ceaselessly in the midst of the pressurization period fulfilling a strain of 6.7% in around 1 s.

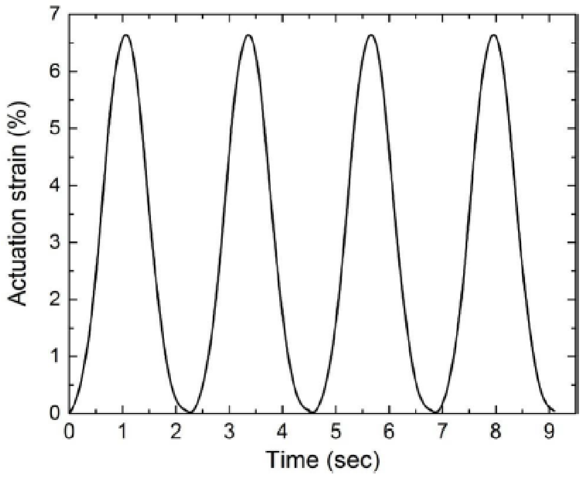

Figure 1.7. Isotonic actuation test under constant air pressure (0.66 bar) and given load of 12mN;

The inert drive verses withdrawal strain test was as well performed for three particular input weights to investigate the hysteresis ponders of this present-day muscle. The greatest inactive drive and compression strain of 275 mN and 2.1%

separately, were accomplished with input weight of 0.45 bar. It wasn't conceivable to perform the try for higher weights because it caused a few harms to the muscle. As it were low-pressure input of 0.66 bar was utilized to get isometric and isotonic charts in this chapter and this brought a result of altogether less vibration delivered by discuss pump.

The calculated power per mass indicates that, the muscle produces the maximum power per mass of 0.036 W/kg after just 0.85 seconds. The calculated power per mass declined once the injection of the air was stopped. Figure 1.8 appears that the whole of dormant drive and compression strain increase with extending the input weight comparative to HAM systems displayed.

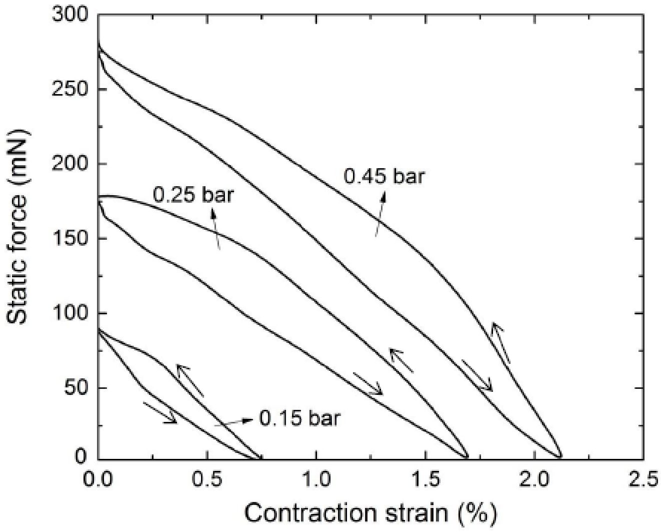

Figure 1.8. Typical static force and contraction strains emphasizing the role of input pressure and illustrating the hysteresis phenomenon for three different input pressures.

2 Kinematics analysis and optimization of the exoskeleton's knee joint

2.1 Basic concepts of exoskeletons. Types. Exoskeleton purposes

In science the term "exoskeleton" is utilized to depict the external inflexible structure of a creepy crawly or shellfish. Within the mechanical field, exoskeletons are the outside inflexible structures that allow bolster to the individuals engine capacities. Exoskeletons incorporate an engine control framework that gives portion of the vitality to the appendage development, and makes a difference the client to move and realize exercises, such as carrying weight. It permits coordinate transmission of the mechanical control and data signals. In this manner, it must be movable or versatile to diverse human body joints, with the objective of adjusting the rotational centers. Special aspects as security, robustness and the robotic mechanism ability should be considered.

Actuators are responsible for generating movement of the elements that forms the exoskeleton. In robotics, an actuator's classification is based on its power source: pneumatic, electrical or hydraulic. Table 1 displays a summary of differences in the basic characteristics of actuator types:

Table 1- Actuators types

Actuator type	Advantages	Disadvantages
Pneumatic	Low cost Fast Simple Robustness	It requires a special installation Noisy
Hydraulic	Fast High load capacity Stability against static charges	It requires a special installation Difficult maintenance Expensive
Electrical	Precise and trustable Noiseless Easy control Easy installation	Restricted power

The selection of the actuator will depend upon the following factors: cost, velocity, control, power, precision, weight, volume, maintenance and security.

Drives are another imperative issue when creating exoskeletons. Pressure driven barrels are very capable and exceedingly precise, but they are overwhelming and utilize a huge number of tubes and hoses. Pneumatics is simple, but the method of taking care of developments is unsteady, since compressed gas is springy.

On an electronic basis, new servos are being developed, which will later include magnets in their work and provide completely accurate movements, using a small amount of energy and at the same time small size. The problem of flexibility will be helped by designers of spacesuits, as well as with the adjustment of the size of the suit.

Another problem encountered during the design of the exoskeleton is the management and elimination of unnecessary and unnecessary movements. The speed of the reaction of the parts of the costume to the movements of the user is also important. If desynchronization of actions occurs, then this will lead to a serious health effect. That is, the exoskeleton will have to “feel” and even predict human behavior. ReWalk (figure 2.1) is a wearable robotic exoskeleton that provides powered hip and knee motion to enable individuals with spinal cord injury (SCI) to stand upright, walk, turn, and climb and descend stairs.

Figure 2.1- REWALK Exoskeleton

Japanese robotics maker Cyberdyne made a good impression. The goal of this project is to help paralyzed people. It is designed for everyday use, for constant work with weights, for the elderly.

These days, special-purpose exoskeletons are picking up increasingly notoriety. For illustration, the Chairless Chair exostula was illustrated, which permits you to sit whereas standing. Lockheed Martin and Daewoo freely displayed exoskeletons for specialists within the shipbuilding industry, empowering specialists to hold devices or loads weighing up to 30 kilograms.

An on-board microcomputer with a touch control system monitors the movements of the soldier and sends information to the exoskeleton, which increases human capabilities with the help of motors. The military is becoming incredibly resilient. So far, the novelty is not used in combat, but is used in test mode. Tests will help to understand how HULC affects the condition of fighters. With a titanium frame, heavy weight is transferred directly to the exoskeleton body. Perhaps the exoskeleton will also be used for civilian heavy loads, as well as to help the paralyzed walk again.

Of course, exoskeletons are the most complex technologies that a person has yet to master, but the future lies with them. Exoskeletons may become an integral part of our lives. Exoskeletons are used in many fields of science and technology, and there are quite interesting fields of application of exoskeletons in medicine and armaments of countries. The exoskeleton repeats human biomechanics for a proportional increase in effort during movement.

In most cases, exoskeletons are only demonstrative options and they still have to pass tests for stability, safety and many others, they will be improved many more times before they go into production.

The actuator and transmission play a dominant role in determining the dynamic performance of O&P devices. Muscles make up a significant portion of a biological limb's mass and also determine its general shape. In trying to duplicate the form and function of a limb it therefore makes sense to use actuators that are similar to natural muscle. Whereas it isn't conceivable to copy common muscle in each respect, we do have to be coordinate those characteristics of normal muscle that give for strong and versatile movement as well as those variables that influence cosmesis and consolation. The going before areas depict the significance of copying certain key highlights of common movement almost a joint. In specific, common muscle is more than fair an engine (drive and movement maker). Muscle is additionally a vitality capacity gadget (spring) and an vitality safeguard (damper). In addition to optimizing the metabolic economy of walking, the energy storage and absorption characteristics (and the ability to modulate those parameters) help a person respond to unknown disturbances, much like the suspension system of an automobile. All these functions are integrated to produce the desirable characteristics of natural walking or other gaits. Strictly speaking, some of the elasticity and damping of natural muscle is borne by the tendons that attach the muscles to the skeleton. For convenience, we will talk about "muscle" as including the function of the tendons. Beyond the stiffness, damping, and force and stroke output capabilities, as well as the cosmetic and comfort issues, it is important to note that biologists and engineers do not yet know all the features of muscle that might be required for natural motion. For case, muscle has exceptionally nonlinear time-varying behavior that may be imperative. Be that as it may, at a least we ought to be able to duplicate the control yield, constrain, stroke, flexibility, and damping (or vitality retention) of normal muscle.

While in theory a suitably fast and powerful actuator acting through a mechanical transmission could use closed-loop feedback control to imitate the performance of natural muscle, such as the series elastic actuator described in the previous section, actuators that share the inherent properties of muscle can be lighter, simpler and offer a more natural look and feel. The requirement for a "natural" look and feel is important to the goal of making the artificial or assisted limb feel integrated with the body. Such actuator requirements are not typically considered in robotic or dynamic machinery applications when actuators are selected. These requirements include completely quiet operation, soft feel, and an external envelope (size and shape) approximating that of a natural limb. In addition, cost is very important. The cost of some shape memory alloys, piezoelectric, and magnetostrictive materials could prevent their use in applications such as lower limbs where large amounts of material are required. Many actuator materials and devices have been put forth as "artificial muscles." Pneumatics and hydraulics (including soft-bodied actuators such as the "McKibben Muscle" can imitate much of the performance of natural muscle and have a shape and feel similar to natural muscle, but they are noisy, difficult to control, and require a separate pump to provide the fluid energy.27 Most typically it is desired to use actuators that can be powered and controlled directly by electricity. Existing technologies are all lacking in some way. Shape memory alloys, while strong with high energy density, are slow and inefficient. Piezoelectrics are fast and efficient but are stiff with a low peak strain. Electromagnetic motors, by far the most common actuator in existing robotic, prosthetic, and orthotic devices, do not offer an adequately high peak or average power output, resulting in devices that are heavier than desired. Furthermore, electric motors achieve maximum power output at high speed and therefore require a high-ratio, nonbackdrivable gearbox or ballscrew in order to produce the speeds needed for limb motion. Since a highly geared system cannot reproduce the compliance of natural muscle, it is necessary to include yet additional elements to provide for muscle-like features, such as the series spring in the series-elastic actuator described earlier. While the functionality of the resulting actuator is good, the mass and unnatural noise of the transmission mechanism are unattractive. For orthoses in particular where the mass of the natural limb remains, minimizing the excess mass as well as bulk of the actuator is critical.

2.1.1 Control system

The framework incorporates a various leveled control structure composed of a human movement deliberate acknowledgment framework (HMIR) at high-level. At that point, for interpretation of the user’s movement purposeful for a wished state for ALLOR, the controller incorporates at the mid-level a limited state machine (FSM), which sets the control methodology comparing to the recognized movement course. At last, an induction, speed and a relative necessarily (PI) controller are dependable for realizing the wished development at low-level. The low-level controller sends the commands to the actuators, which move the structure of the mechanical exoskeleton. The following sections describe details of the components of the proposed system.

The active knee exoskeleton, termed ALLOR is composed of an active knee joint and a passive hip joint, which moves itself in the sagittal plane during the gait. It was built for knee rehabilitation in both seated position and walking, and provides both mechanical power to the knee joint and feedback information related to the knee angle, interaction torque, and gait phases. ALLOR has a mechanical structure of aluminum (type 7075), which is attached to the user’s joints. It was built using active orthoses design-criteria for lower-limb devices for assistance and rehabilitation reported by (Villa-Parra et al., 2015). It is mounted on the left leg of the user, and is adaptable to different anthropometric setups, which include heights of 1.5 to 1.85 m and weights from 50 to 95 kg. To ensure a correct alignment during operation, a backpack and rigid braces are used. The backpack consists of shoulder straps and a belt that wraps around the wearer’s waist. The belt is balanced at the hip joint to maintain the orthosis structure. In expansion, the rucksack was adjusted to put the sEMG terminals at trunk, which incorporates a free space to get to them at the lumbar region of the client, and a cover for the zone. The unbending braces are secured with a delicate fabric, and are movable through velcro straps to diverse breadths and lengths of the user's thigh and shank. The total weight of ALLOR is 3.4 Kg, including 0.8 kg of the backpack.

The hip joint has a manual flexion-extension angle regulator (0 to 80°). Although this joint is not active, its regulation, according to the user requirements, allows establishing a safe range of motion.

Figure 2.2 shows the block diagram of the proposed system, which includes our knee exoskeleton termed ALLOR (Advanced Lower Limb Orthosis for Rehabilitation), developed at Federal University of Espirito Santo (UFES/Brazil).

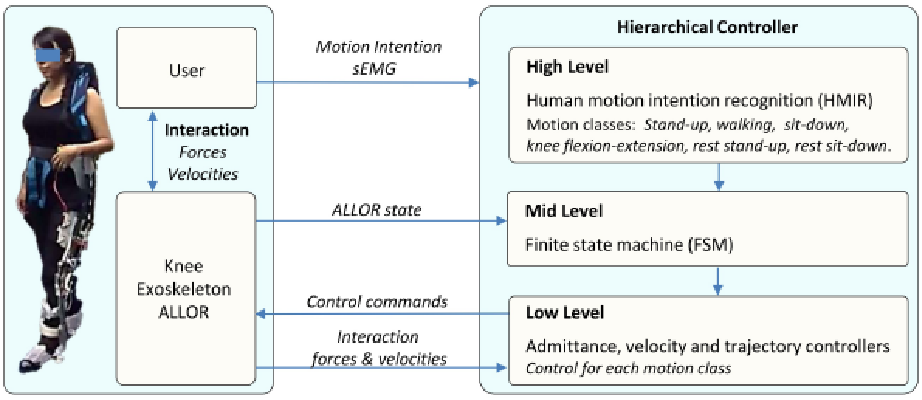

Figure 2.2. Block diagram of the proposed system.

The output of the HMIR is used to select a state with a finite state machine (FSM) defining both wished admittance and parameters for the velocity and trajectory low-level controllers to command the knee exoskeleton ALLOR. The components of the active knee joint are a brushless flat motor (model 408057), a Harmonic Drive gearbox (model CSD-20-160-2A-GR) and an both digital and analog PWM servo-drive (model AZBH12A8). Additionally, ALLOR is equipped with a strain gauge arrangement (Wheatstone bridge configuration), which measures the torque produced by its interaction with the user. A precision potentiometer (model 157S103MX from Vishay Spectrol) is used as an angular position sensor to measure knee angles, and an instrumented insole with four FlexiForce A401 resistive force sensors is used for both measure plantar pressure and to recognize gait phases. ALLOR also uses Hall Effect sensors inside the motor to compute angular speeds of the actuator.

The acquisition hardware was attached to a mobile platform in order to follow the subjects during the test. Thereafter, the sEMG data were processed off-line using Matlab 2014b. The HMIR system was validated for both lower-limb and trunk muscles. During the supervised learning, the classifi ers were trained combining the fi rst six trials from the sequential experiment with four trials from the random experiment. For validation, the remaining four and two trials from the sequential and random experiments were considered, respectively.

Analysis for each subject S1 to S10 was performed independently. To assess the effect of using muscular groups of the trunk to accurately recognize lower-limb motions, statistically signifi can't difference between these two muscular groups were evaluated using the Wilcoxon rank sum test, as the data did not pass the normality test (one sample Kolmogorov-Smirnov). Figure 2.2 shows the placement of electrodes and the execution of the motion classes during tests.

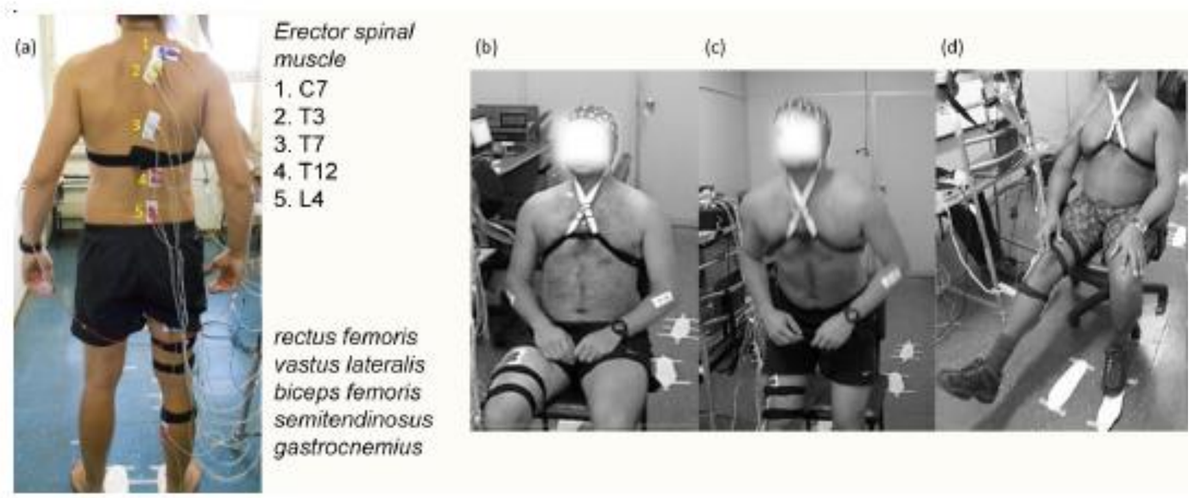

Figure 2.3. Placement of electrodes and the execution of the motion classes during tests.

The electrodes on the trunk are marked at the picture with numbers. (b)-(e) motion classes during tests: Rest in Sit-Down position (RSD), Stand-Up (SU), knee Flexion-Extension (F/E), and Walking (W), respectively. In order to both follow the subject during walking, and control the stride length, a mobile platform with the acquisition equipment and footprints on the floor were employed, respectively.

2.1.2 Controller test

Two healthy female subjects (25 years; height 1.60 m; weight 72 kg and 22 years; height 1.69 m; weight 70 kg) without lower limb injury or locomotion defi cits were selected to participate. At the beginning of the experiments, the subjects were given 5 to 10 min to familiarize with ALLOR. The recording of the trajectories SU and SD was performed at the beginning of the experiment with the user employing a walker. The velocity profi le F/E was generated by the algorithm previously shown in Figure 2.3, with q_{min} =20°, q_{max} =75°, downtime =0.5 s, uptime =5 s. To assist the gait, the gain G for initial contact, mid-stance, terminal stance and swing gait phases were: G1= 0.4 UW, G2 = 0.7 UW, G3 = 0.2 UW and G4=0.1 UW, respectively, where UW is the user weight in Kg.

A sequence of the motion classes was conducted to demonstrate the ability of the controller to perform the movements with the user employing a walker. Then, a test to evaluate the SC with the admittance adjustment during gait was realized with the subjects walking a distance of 10 m using ALLOR. Three trials were performed with the acquisition hardware attached to a four-wheel walker, in order to offer support and to have a mobile platform during the test.

To survey the impact of utilizing ALLOR amid tests, information from the subjects, related to knee point, torque, induction tweak and stride stage were gotten. At that point, most extreme point, most extreme torque, position stage rate and walk cycle length were analyzed.

2.2 Elements for implementing work with exoskeleton

The plan and determination of the actuators were based on ordinary values of torque and control of each joint along the walk cycle amid typical stride (not obsessive) at typical speed. A ponder of distinctive conceivable candidates for actuators was assessed. The foremost significant criteria to choose the incitation innovation to drive the human joints were the particular control (proportion of actuator control to actuator weight) and movability. Straight pressure driven and pneumatic actuators have tall control thickness, but a few works recommends that the utilize of electric engines give a diminishment in control utilization amid walk.

Also, hydraulic and pneumatic actuators are usually bulky and cannot be easily controlled. DC motors meet the criteria of necessary power with a compact and portable solution for wearable devices. Within the DC motors category, brushless motors offer several advantages for wearable devices, including higher efficiency, more torque density, increased reliability, reduced noise, longer lifetime and reduction of electromagnetic interference. Based on these important characteristics, brushless DC motors were selected. Moreover, the selected motors are flat type. This characteristic brings the possibility of placing the motors coaxially with the joints and maintaining a small volume on the side of the leg. As the exoskeleton joints need more torque and less speed than DC motors can provide directly, a possible solution for increasing torque and reducing the speed is coupling a gearbox to the motor shaft output. To achieve a lightweight and a small volume solution, strain wave gears were selected as a gearbox.

The joint motors are driven by a PWM (Pulse Widht Modulation) servo drive (Advanced AZBH12A8) designed to drive brushless DC motors at high switching frequency. The AZBH12A8 is completely secured against over-voltage, overcurrent, over-heating, invalid commutations and short-circuits. Its employments Lobby sensors criticism to commute stages and in this way control the engine speed. With a compact estimate, 63.5 x 50.8 x 16.8 mm, and as it were

86 grams, it works in a fourquadrant mode, which permits it to recover control when engines are being decelerated. An analog line gives to the drive the speed set point. Each drive, can drive a single joint. A Lithium-ion battery pack of 22.5 VDC and 6.8 Ah is used to power the exoskeleton. The battery pack weights 960 grams and measures 180 x 70 x 40 mm. This small power pack is expected to run the exoskeleton for about one hour of continuous walk.

The exoskeleton is equipped with two types of sensors: kinematic and dynamic.

Each joint is prepared with a exactness mechanical potentiometer utilized as an precise position sensor. The 10-k potentiometer utilized encompasses a tight linearity, i.e. 0.25%, and long rotational life. Its stainless-steel shaft is coupled to a toothed pulley and a toothed belt is utilized to transmit the joint movement. This maintains a strategic distance from slippage and so a misfortune of reference position. This sensor can be seen in figure 2.4. These sensors are planned to degree the torque delivered by the interaction between the subject's appendage and the exoskeleton. Four strain gauges are connected in a full Wheatstone bridge configuration to enhance the measurement accuracy and insensitivity to temperature variations.

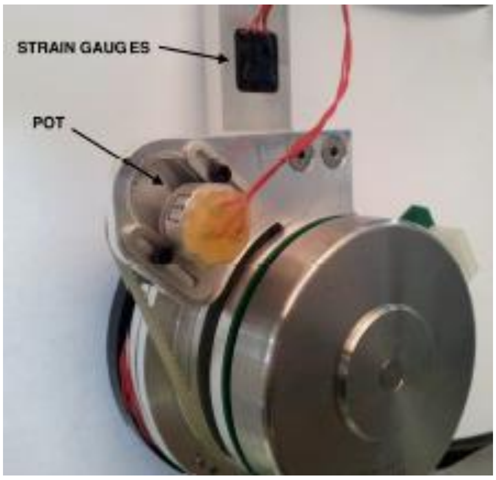

Figure 2.4. Position and interaction torque sensors in the hip joint.

The bridge is energized with 5 VDC. A custom-made electronic circuit was created to adjust the bridge for invalid point estimation and open up the yield 100 times. Thus, the output signal is in a range that allows torque measurements from –40 to +40 Nm. This range was chosen based on the maximum continuous torque of the actuators. A calibration constant was obtained by using a set of calibrated weights and minimizing with a least square algorithm.

2.3 Knee static force analysis

In spite of the fact that the comes about for quadriceps muscle drive are appropriate to ordinary bipedal movement, it was regarded basic for this inquire about to create an explanatory biomechanical demonstrate in arrange to approve PAMs for fueled transfemoral prostheses. Knee inactive drive examination amid walk was conducted by creating a 3D Strong Works show of a human subject utilizing anthropometric information from the writing. In this way, the measurements of the demonstrate appeared in figure 2.5 are relative to those of a standard human body. To enough assess the quadriceps, constrain and hence the minute approximately the knee, constrain investigation was performed at five percent interims amid the position stage of the stride cycle for level strolling, stair rising, and sit-to-stand development.

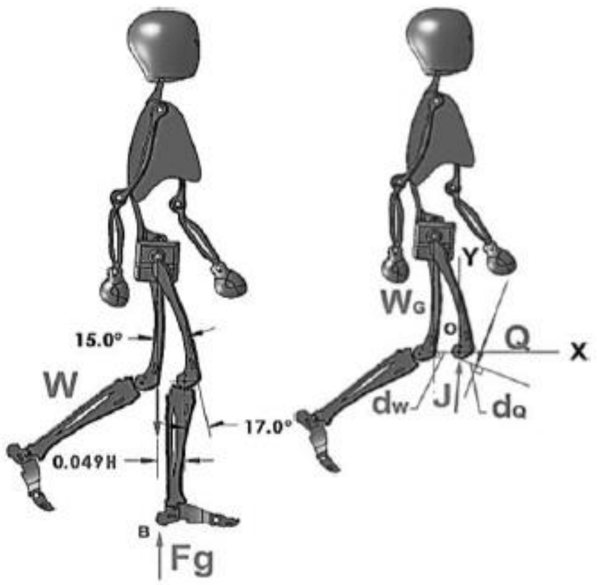

Figure 2.5. Free-body diagrams of subject during level walking developed in SolidWorks.

The hip, knee, and ankle joint angles from a previous study were used for the stance phase of the gait cycle at five percent intervals. Using this information and the developed 3D model, two-dimensional (2D) sagittal free body diagrams were developed. The first free body diagram of figure 2.5 assumes single support and consists of the entire subject and two external forces, namely the body weight *W* and the ground reaction force *Fg*. For static equilibrium, it was assumed that the body weight force is aligned with the ground force reaction and thus the body weight does not generate any moment about the foot center of pressure. In figure 2.5, the second free body diagram consists of the entire subject without one lower leg, insteading showing three external forces, namely the femoral-tibial contact force *J*, the quadriceps muscle force *Q*, and the body weight minus the lower leg weight *Wg*.

With reference to figure 2.5, *O* corresponds to the femoral-tibial contact point and the center of rotation of the knee joint, *dW* is the perpendicular distance between the body weigh vector *Wg* and point *O*, and *dq* is the perpendicular distance between the quadriceps muscle force vector *Q* and point *O*.

For each knee flexion angle, dq was obtained from the literature [8]. The location of the body center of mass, and thus dw, was also obtained from the literature. Applying an equilibrium condition at any point of the gait cycle, the quadriceps muscle force Q is determined as:

$$Wg = BW - W\,\mathrm{l} \qquad (2.1)$$

where $BW$is the total body weight

$W_L$is the weight of the lower leg. From a previous study:

$$Wg = 0{,}939BW \text{ or } W\,\mathrm{l} = 0.061\mathrm{BW}$$

For a sample calculation, arbitrarily picking 10% of the gait cycle and assuming single support, according to a previous study [8], dq is equivalent to 0.04601 m for a knee flexion angle of 17.6°. With reference to Fig. 10, dw is 0.1322 m for a subject 1.7 m in height. Applying equilibrium conditions about point O with positive moments in the clockwise direction yields:

$$\sum M = 0 \qquad (2.2)$$

$$Q = \frac{w_{q \times d_{wg}}}{d_g} = \frac{0.939BW * 0.1322}{0.0.4601} = 2.698\ BW$$

The required quadriceps force for a subject with a body weight of 75 kg (736 N) is thus 1985.1 N.

Referring to the same point of the gait cycle once again, but assuming the more realistic scenario of double support, Fg from the contralateral leg will contribute to the net moment about the point O on the knee joint of interest. The center of pressure of the contralateral foot is estimated to occur mid-foot. Assuming that the transfer of weight from one foot to another occurs linearly between 0 to 15% of the gait cycle, Fg is found to be approximately 48 N for a 75-kg subject and occurs at a distance dg of 0.3541 m from the point O. Applying an equilibrium condition at that point with positive moments in the clockwise direction, the quadriceps force Q is determined as:

$$Q = \frac{w_{q \times d_{wg} - F_q \times d_g}}{d_q} = \frac{690.87 * 0.1322 - 48 * 0.3541}{0.04601} = 1612.80\ N$$

This process was repeated for every 5% increment of the stance phase of the gait cycle. The results are shown in figure 2.6. The maximum calculated quadriceps forces are 3792 and 1647N at the beginning of the gait cycle for the single and double support scenarios, respectively. The quadriceps force obtained from the biomechanical model based on the double support assumption more closely matches the results obtained.

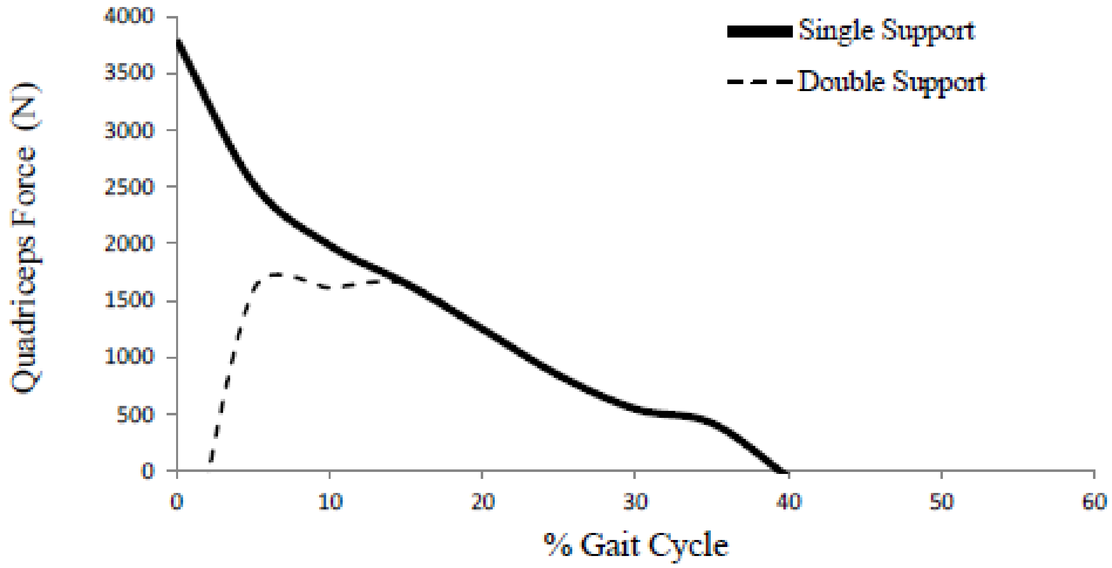

Figure 2.6. Quadriceps force for level walking during stance phase of gait cycle for single and double support.

The maximum moment contributed to the knee joint by the quadriceps muscle during the stance phase of the gait is:

$$M = Q \times d_q \tag{2.3}$$

$$M = 3792 \ \times 0.02966 = 112.47Nm \ \text{(single support)}$$

$$M = 1647 \ \times 0.0475 = 78.25Nm \ \text{(double support)}$$

Performing clinical gait analysis using a 3D musculoskeletal model experimentally determined the knee joint moment throughout the gait. According to their study, for a subject with a body weight of 75kg (736 N), the maximum moment about the knee joint is approximately 56.9 Nm, which occurs at 16.5% of the gait cycle. While it is hard to compare the net knee, moment obtained experimentally and the analytical moment calculated based on one muscle contribution.

3 Technical part of the work

3.1 Components for assembling a prototype of an experienced muscle and control system

3.1.1 Microcontroller

When choosing a microcontroller to control the process of supplying and outputting pressure to the artificial muscle, the Arduino Mega 2560 was enough for me, since it was possible to power the valves of figure 3.5 and control the relay module figure 3.6 through the digital outputs. And so writing code for the operation of the circuit would be convenient, in comparison with Raspberry PI.

Arduino Mega 2560 (figure 3.1) is a device based on the ATmega2560 microcontroller. It includes everything necessary for convenient work with the microcontroller: 54 digital inputs / outputs (of which 15 can be used as PWM outputs), 16 analog inputs, 4 UART (hardware transceivers for implementing serial interfaces), a 16 MHz quartz resonator, USB connector, power connector. To start working with the device, simply supply power from the AC / DC adapter or battery, or connect it to the computer via a USB cable.

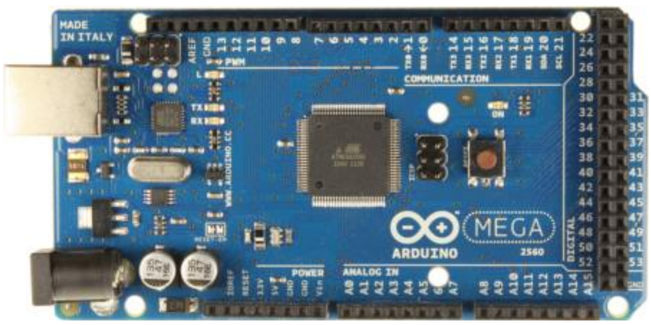

Figure 3.1 - Arduino Mega 2560

Table 3.1 – Arduino characteristics

Microcontroller	ATmega2560
Working voltage	5V
Supply voltage (recommended)	7-12V
Supply Voltage (Limit)	6-20V
Digital inputs / outputs	54 (of which 15 can be used as PWM outputs)
Analog inputs	sixteen
Maximum current of one output	40 mA
Maximum output current output 3.3V	50 mA
Clock frequency	16 MHz

Arduino Mega can be powered from USB or from an external power source - the type of source is automatically selected. An external AC / DC adapter or battery / battery can be used as an external power source (not USB). In case of power supply from the accumulator / battery, its wires must be connected to the terminals Gnd and Vin of the POWER connector.

The power pins located on the board are listed below:

- The voltage supplied to the Arduino directly from an external power source (not connected to 5V from USB or other stabilized voltage). Through this output, you can both supply external power and consume current when the device is powered by an external adapter;

- This output receives 5V from the voltage regulator on the board, regardless of how the device is powered: from the adapter (7-12V), from USB (5V) or through the VIN pin (7-12V). It is not recommended to power the device through the 5V or 3V3 terminals, since in this case the voltage stabilizer is not used, which can lead to board failure;
- GND is normally at 0 volts point for a power supply and circuit.

3.1.2 Actuating the artificial muscle

The choice of a compressor (figure 3.2) is one of the most important tasks in the development of artificial muscle, the performance of manufacturing a part, the economic use of production facilities, electricity and, as a result, the cost of the product depends on its correct choice. Equipment on the designed site should be as versatile as possible.

Figure 3.2 - Air compressor

I chose an air compressor Cyclone KS-303 piston, with the following characteristics:

Table 3.2 - Air compressor characteristics

Voltage	12-13.5 V
Power	170 watts
Amperage	14 A
Performance	35l / min
Maximum pressure	7/10 kg / cm2

3.1.3 Power Supplies

To implement the prototype of an artificial muscle, 2 different power sources were needed. One of them was needed to power the valves through the Arduino

Mega2560. This power supply (figure 3.3) has the following characteristics: input voltage 100-240V, output 12V / 4A.

Figure 3.3 - Power supply for Arduino Mega 2560

I also used a transformer charger (figure 3.4) to work with an air compressor.

Having a voltage of 6-12V at the ends and a current strength of 20A.

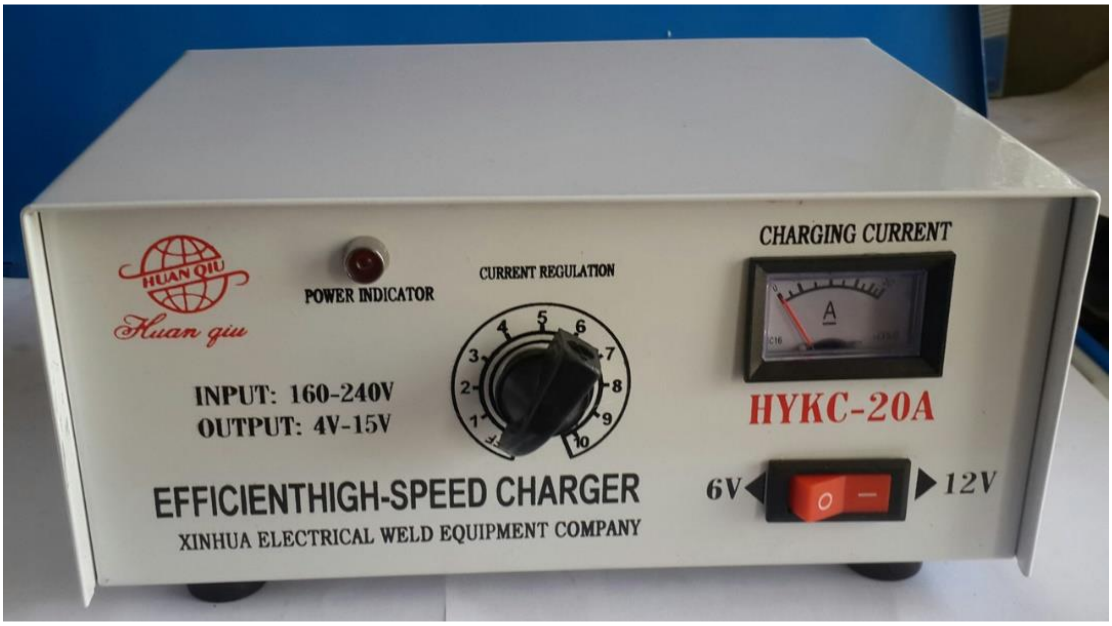

Figure 3.4 - Transformer charger

3.1.4 Devices for controlling the flow of air supplied to the artificial muscle

To supply and pump pressure in the right direction, I used an electrically controlled valve (figure 3.5), which is in a normally closed state.

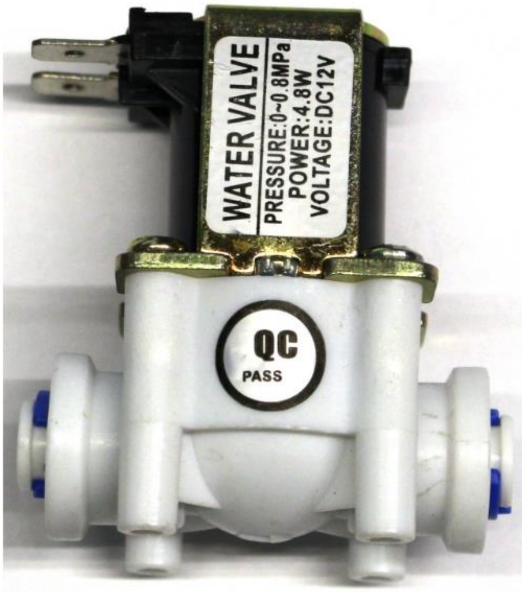

Figure 3.5 - solenoid valve

The power control of the valves is done through a relay module (figure 3.6) designed for Arduino. The principle of operation of the relay in Arduino turns on or off external devices, in a certain way closing or disconnecting the separate electrical network into which they are connected.

Figure 3.6 - Relay module

3.2 Assembly of elements for the process

I composed the program in such a way that at to begin with the flag goes to one hand-off, at that point the flag switches to another. So it turns out that the solenoid valves work in turn, each 10 seconds. I composed such a program since when discuss passes through one valve, the other must be closed, as the discuss can exit and my muscle will not blow up. When exchanging to another valve, that's, after 10 seconds, the discuss goes out, and my muscle is liberated from the discuss stream and liberated. The program can be seen in figure 3.7:

sketch_may31a §

```
int RELAY = 7;

void setup()

{

pinMode(RELAY, OUTPUT);

}

void loop()

{

digitalWrite(RELAY, HIGH);

delay(10000);

digitalWrite(RELAY, LOW);

delay(10000);

}
```

Figure 3.7 - Program code

Hence, having associated all the gadgets, my work is put into activity (figure 3.8).

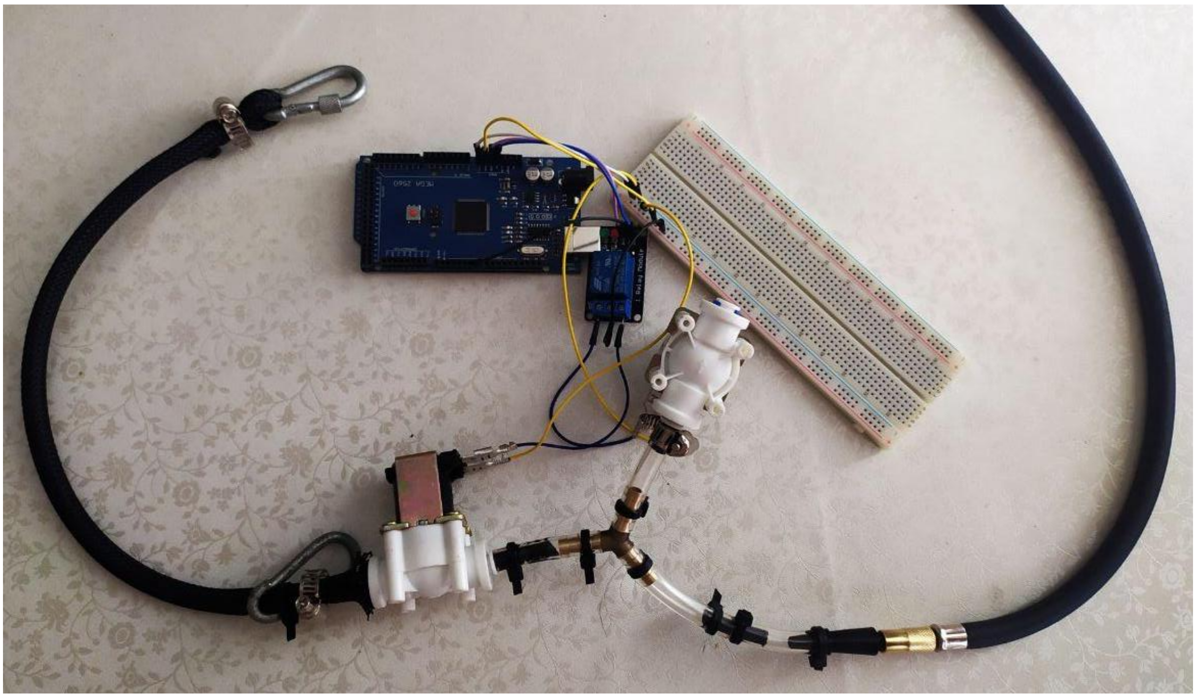

Figure 3.8 - Assembled prototype

3.3 Making an experiment

And so, I conducted experiments on artificial muscle. To start, I took a muscle 35cm long and measured its length after applying air.

Figure 3.9 - measure muscle

It turned out that the muscle contracted from 35 cm to 28.5 cm, that is, it decreased by 6.5 cm.

Next, I attached the load to the muscle (figure 3.10) to see how the muscle will contract. I hooked a bottle filled with 1 liter of water.

Figure 3.10 – length changing with load

There we can see that, muscle declined to 8 cm, from 44 to 36 cm. The third experiment was with short muscle (figure 3.11). This muscle also attached with load.

Figure 3.11 – short muscle

There we seeing that muscle decreased to 3 cm, from 19,5 to 15,5 cm.

After that three experiments, I had researched that all of artificial muscles changed their length to probably 18% from initial value (6,5 is 18,5% of 35, 8 is 18,1% of 44, 3is 18,4% of 19)

During the air supply, the maximum pressure (figure 3.12) of the compressor was 50 bar. This tells us that my artificial muscle can no longer grow and remains at this pressure.

Figure 3.12 – Pressure value

3.4 3D model in Solidworks

I made a model (figure 3.13) of knee exoskeleton in the Solidworks program.

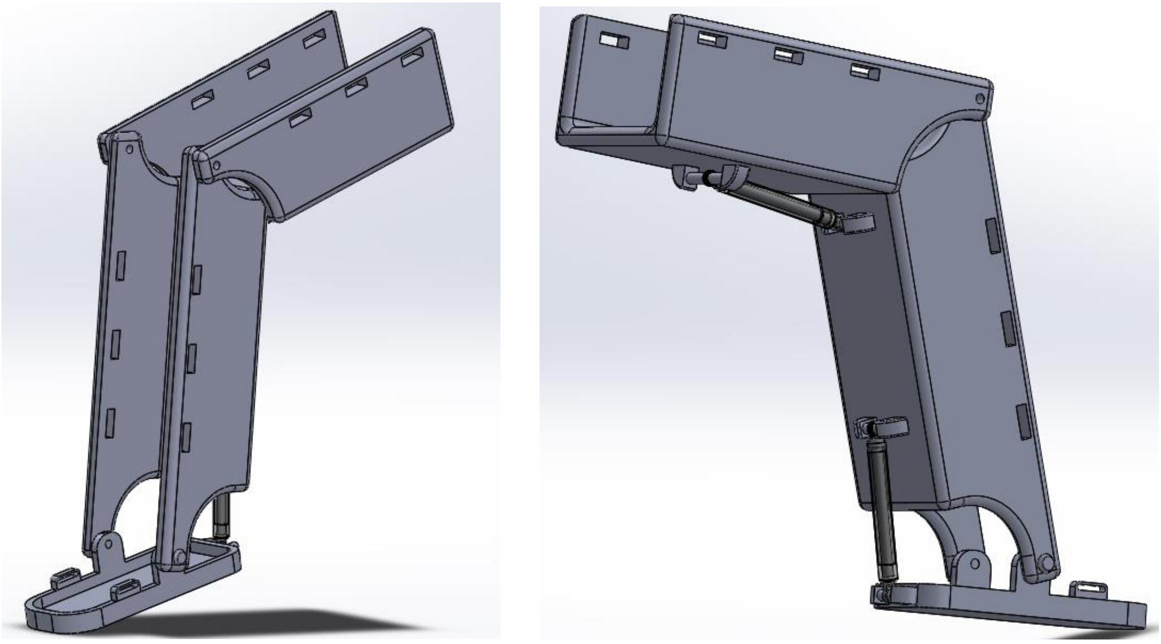

Figure 3.13 – 3D model

I've done Flow Simulation in Solidworks. I've calculated the pressure and temperature changing in the graphs. It's shown in Figure 3.14:

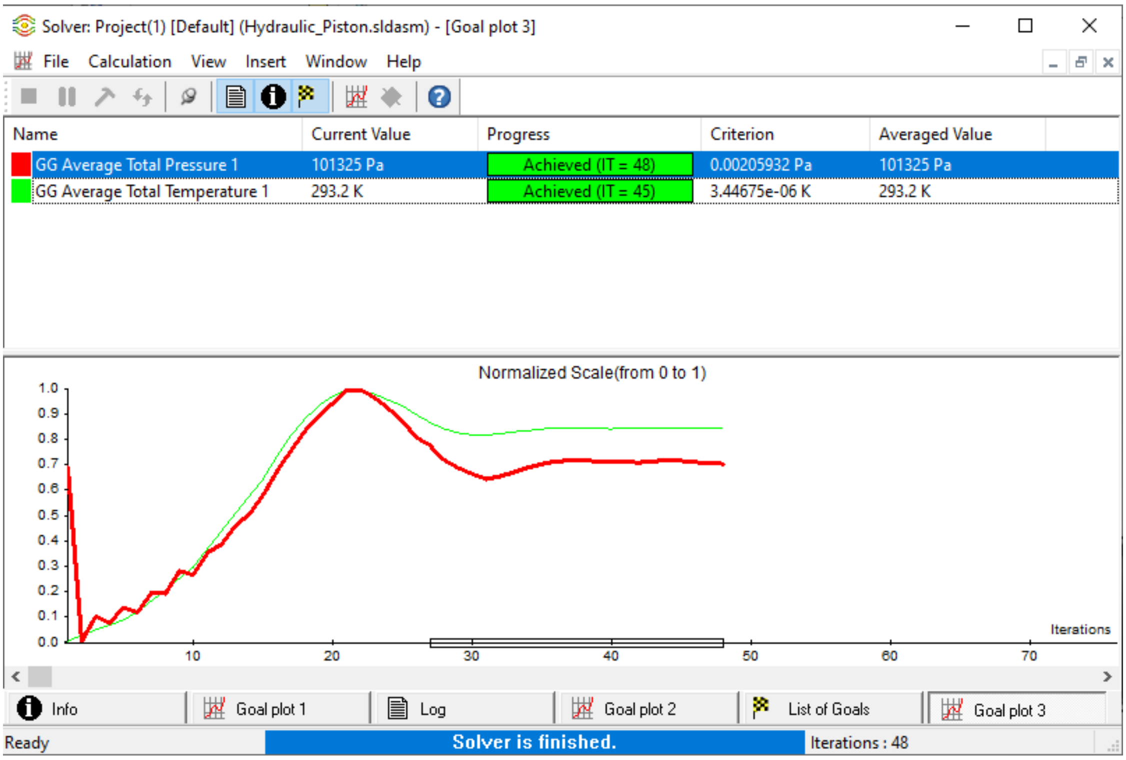

Figure 3.14 – Temperature and pressure graph

After that, I've done simulation of air flow. There's shown the value of pressure and air's direction

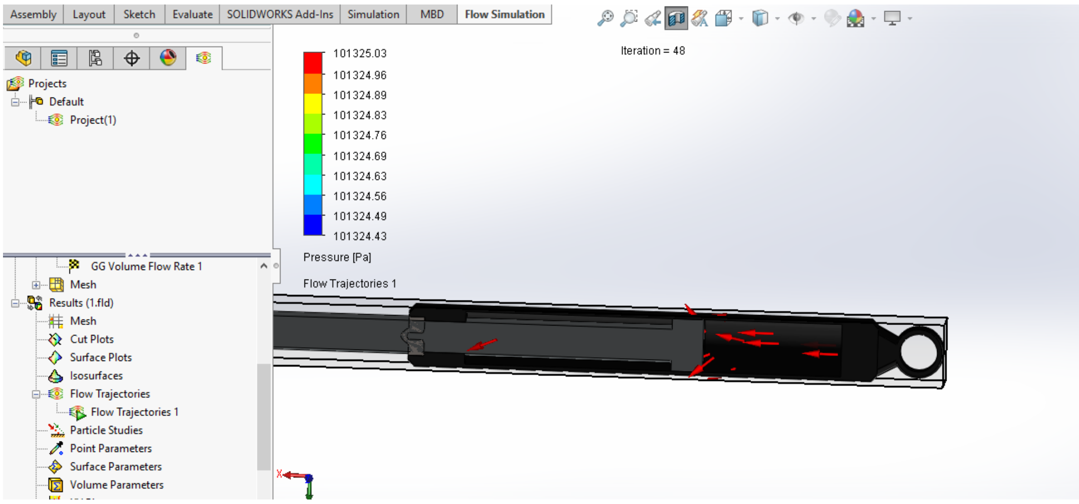

Figure 3.15 – Air direction and pressure value

4 Life safety

4.1 Analysis of working conditions

The task of working conditions is to compare existing dangerous and harmful production facts with the requirements of relevant standards, norms, rules and other documents on labor protection.

Sufficient illumination of workplaces, technical serviceability of the equipment used, provision of fire safety, as well as the creation of a normal microclimate in the workplace - the conditions necessary for the organization of a comfortable workplace that meets the safety standards.

The room is located in the city of Almaty. This region is characterized by a variety of weather conditions in different periods of the year. Geographical position, the relief of the surrounding area are factors that make the change in weather conditions lightning fast. In this regard, the workplace must create conditions for air comfort. These conditions are formed depending on the systems of aspiration, heating systems, ventilation and air conditioning. Proper management of these systems will create satisfactory working conditions.

The amount of the working equipment in the room is 4. The air conditioning is located near the window. Fire extinguisher is carbonic acid, because of the work character with big number of electronic devices. It is located near the exit from the room. Working hours are from 9a.m to 6p.m.

The dimensions of the audience's working diagram: the height of the room is 3 m, the width is connected changed to 3 m, length - 4 m. The total provision of the premises received is a minimum of 19.25 m2. Glazing rooms number double with plastic binding, taking the dimensions of digital windows 1700x framing1800. By the category of visual control systems, the room belongs to the IV satisfaction of the category with the smallest aero visual object size attenuation discrimination from 0.5 to 1 mm. Plan of working room in figure 4.1:

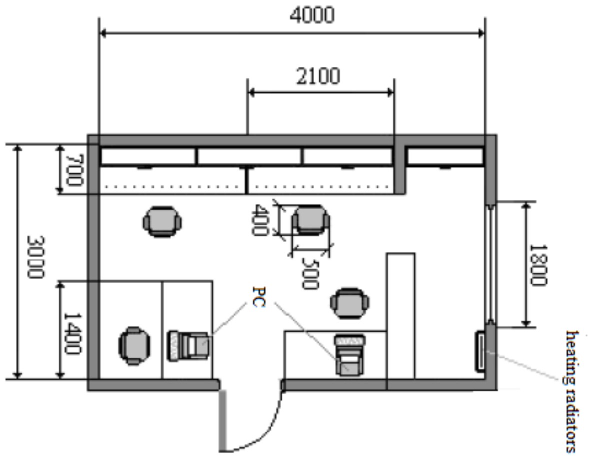

Figure 4.1 – Working room plan

Simultaneously in the room are working 2 engineers.

In the office there are 2 workplaces of software engineers with all the adjacent equipment. Room area S = 3x4= 12 m^2, Volume - V_{contr} = 12x3 = 36 m^3. Therefore, per person has an area of 12/2 = 6 m^2 and a volume of 36/2 = 18m^3.

This is more than the minimum area and volume per employee set by the norms (volume - at least 15 m^3, area - at least 4.5 m^2).

Used equipment:

- 2 PCs;
- 2 scanners.

It is assumed that 2 employees will work in the room during the daytime: a system administrator and programmer.

Undesired work performed by enterprises belongs to the category of lungs followed by work of workers (category Ib),
performed in a reduced sitting position (GOST calculation 12.2.032-78). attenuation working touch height surface: 725 mm; personal seat height requires: 420 mm (GOST 12.2.032-78)

Modern air conditioning systems allow for various manipulations with air. Changing the parameters of cooling, heating, cleaning, setting the humidity is made by easy adjustment. Such systems are very intelligent. The user does not need to pay attention to monitoring these parameters. The system independently monitors these parameters and also independently supports them within the necessary limits.

In summer, heat input through external structures (walls, ceiling) is usually positive. The calculation is complicated by the fact that the air temperature varies greatly during the day, and the solar radiation further heats the external surface of the building. In winter, heat is lost through external structures. The temperature fluctuations in winter are less, and the heating of surfaces by solar radiation is negligible.

Heat input (or loss of heat) due to the temperature difference depends not only on external conditions, but also on the temperature inside the room.

Calculation of heat quantity

The amount of heat Q_{lim}, transferred by heat transfer through a fence (wall) with area S, having heat transfer coefficient k, is calculated by the formula:

$$Q_{lim} = S * k * (T - t) \quad (4.1)$$

The calculated outside temperatures depend on the region, and the internal temperatures are chosen taking into account the comfort or technological requirements, depending on the purpose of the room.

This formula is simplified and does not take into account a number of factors. In order to take into account, the direction with respect to the sides of the world, solar radiation, heating the walls, etc., it is necessary to introduce corrections into this formula. They are constituent parts of the coefficient Y.

The absorption of solar radiation by the fence depends on the following factors:

Wall colors: the heat absorption coefficient reaches 0.9 for the dark color of the outer walls and only 0.5 for the light walls.

Thermal characteristics of walls: the more massive the wall, the greater the delay in the flow of heat into the room. The thermal load when the massive wall is heated is distributed for a longer time. The calculation is complicated by the fact that the air temperature varies greatly during the day, and the solar radiation further heats the external surface of the building. If the walls are thin and light, then the thermal loads increase and change rapidly when the external conditions change. This requires more expensive and powerful air conditioning.

The heat of solar radiation can significantly increase the heat input into the building (for example, in a store with display windows). The room is transferred to 90% of the sun's heat, and only a small part is reflected by the glass. The most intense heat radiation comes in summer, in clear weather.

Heat input of radiation is taken into account in the heat balance of the building only for summer and transition times, when the outside temperature exceeds +10 degrees.

The heat input of solar radiation depends on the following factors:

- Kinds and structures of fencing materials;
- The surface states (for example);
- Less radiation passes through dirty glass;
- Angle, under which the sun's rays fall to the surface;
- Orientations of the room to the sides of the world (heat losses from radiation through windows facing north are not taken into account at all).

The calculated value of heat input from radiation is taken to be the greater of two values:

- Heat coming through the glazed surface of that wall, which is most advantageously located relative to the heat input or having the maximum light surface;
- 70% of the heat coming through the glazed surfaces of two perpendicular walls of the room.

If it is necessary to reduce heat losses from solar radiation, it is recommended to take the following measures:

- to make a minimum number of light apertures.

Use protection from sunlight: double glazing, whitewashing of glass, curtains, blinds, etc.

When using complex solar protection, the heat input from radiation can be reduced by almost half, and the power of the required refrigeration unit will decrease by 10-15%.

In rooms for various purposes, the thermal loads that occur outside the room (external ones) act mainly; and also, the heat loads arising inside buildings (internal).

External heat loads are represented by the following components:

Heat input or heat loss, which are determined by the temperature difference inside and outside the building.

Temperature difference is determined by the fact that in summer the temperature is positive in the building, because Warm air comes from outside into the building, and in winter everything happens in the opposite way and the temperature has a negative value;

The load also manifests itself in the form of perceived heat through the glazed parts of the building from the sun;

4.2 Calculation of water heating to normalize microclimate parameters

Heating systems to normalize microclimate parameters. Heating in combination with constructive solutions of buildings is designed to provide standardized temperature conditions for normalizing the microclimate of industrial premises.

The complex of structural elements designed to receive, transfer and transfer the necessary amount of heat to all heated rooms is called a heating system. The heating system includes heating appliances, main pipelines for supplying and discharging the coolant, risers, connecting pipes, control valves, air collectors, a boiler or heat exchanger with centralized heat supply, mixing plants and circulation pumps.

Sanitary and hygienic requirements for heating systems are aimed at maintaining a certain and uniform temperature in the premises during the cold season, limiting the surface temperature of heating devices and ensuring their noiseless operation.

Heating systems are divided into two groups: local and central.

Local systems include those in which heat is obtained and used in one room, and central systems include systems designed to heat several rooms or buildings from a single heat center.

Depending on the coolant used, steam, air, water and electric heating are distinguished,

In steam heating systems, the heat carrier is high-temperature steam supplied under high pressure. The disadvantages of steam heating are the high temperature of heating devices up to 373 K (100 °C) and high noise levels. Therefore, its use is allowed in rooms with a short stay of people in them. In rooms with facilities of categories A, B and E (see chapter 16), steam heating is not allowed.

Water heating is most widely used as the most hygienic, silent, economical and perfect in operation. It provides an opportunity to widely regulate the heat supply of the premises depending on the outdoor temperature.

Water heating systems are divided into low temperature with hot water temperature t up to 378 K (105 ° C) and high temperature t from 378 K to 423 K (150 ° C). The calculated return water temperature is 343 K (70 °C).

There are water heating systems with natural and pumping water circulations. Natural circulation is rarely used and only in small detached buildings.

Depending on the power supply scheme, water heating systems are divided into vertical and horizontal, single-pipe and double-pipe with lower and upper wiring. At railway transport enterprises, horizontal single-pipe systems with pump circulation are mainly used for heating industrial premises (figure 4.2).

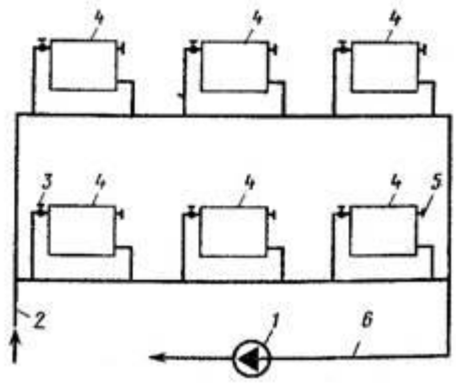

Figure 4.2 – Scheme of a horizontal single-pipe heating system

Where 1 - circulation pump;

2 - hot water pipeline;

3 - control valves;

4 - heating appliances;

5 - air cranes;

6 - return water pipe.

There is a room with an area of 12 square meters 4 (m) * 3 (m) and a height of 3 meters (standard room in a Soviet-era high-rise building):
The first one. what you need to know to calculate is the volume of your room.

Multiply the length and width by height (in meters) (4 * 3 * 3) - and we get the number 36. This is the volume of the room in cubic meters.

The second one. for heating one cubic meter in a standard-built house (without metal-plastic windows, foam insulation, etc. energy-saving measures) in the climatic conditions of Kazakhstan, 36 watts of thermal power are needed.

We find out how much heat we need, for this we multiply our (your) volume V by the number 36:

$$\mathrm{V} * 41 = 36 * 36\,\mathrm{W} = 1296\,\mathrm{W}$$

The resulting figure is the amount of heat that radiators must give out to heat your room. Round it up to 1300.

In our case, we can limit ourselves to a steel panel radiator with a capacity of 1300 watts.

For reliability, it is worth increasing the figure by 20 percent. To do this, we multiply 1300 by a factor of 1.2 - we get 1560. Radiators of this power are not sold, so we round the figure down - up to 1500 watts or 1.5 kilowatts.

That’s all the figure that we need. A radiator of any type: bimetallic, aluminum, cast iron, steel, white speckled and blackish striped will provide us with room heating in any frost possible in our latitudes, if it generates 1500 watts of heat.

For example, a typical fin power of an aluminum or bimetallic radiator with a height of about 60 centimeters is 150 watts. So, we need 10 ribs. Similarly - for standard cast iron radiators type MS-140

To find out the number of heating devices for the entire apartment, we carry out the calculation for each room separately.

Heating of multi-storey buildings is carried out centrally throughout the cold period. But residents of houses, especially panel ones, are not always happy with the temperature in the apartment. The owners themselves try to increase the air temperature in the rooms. They make a simple calculation of the required number of additional batteries and, having bought them, increase the heat transfer area. With the general replacement of old heaters and the installation of new ones, all the more, you need to carefully calculate everything in advance. This will avoid mistakes and unnecessary material costs.

The calculation of the number of sections is carried out according to a simple formula:

$$K = V * \frac{Q_{pom}}{Q_{nom}} \tag{4.2}$$

In this formula, K is the number of sections, Qpom is the set amount of thermal power needed to heat 1 m 3 of the room. This value depends on the type of room: prefabricated house, brick or modern building. Qpom values are given above. Qnom is the rated thermal power of 1 section of the battery. It is indicated in the documentation of the heater. When purchasing such devices, it is necessary to carefully review all technical documentation, the value of thermal power should be indicated in it. Be sure to pay attention to the presence of all the necessary seals and warranties.

For greater clarity, the calculation of the number of sections for a room with an area of 18 m 2 in a panel house can be given. Ceiling height - 2.7 m. The volume of such a room will be equal to 18 * 2.7 = 48.6 m 3. The thermal power required for heating 1 m 3 in a panel house is 0.041 kW or 41 W. The rated power according to the passport data of one section of aluminum radiators is 150-200 watts. Take an average of 180 watts, or 0.18 kW. Further, the calculation will be as follows:

$$K = 48.6 * 0.041 / 0.180 = 11.07 \text{ pcs}$$

Round up to 12 sections.

4.3 Calculation of indicators of the heat state of a human

Human heat transfer with the environment. One of the necessary conditions for the normal functioning of a person is to ensure normal meteorological conditions in the premises, which have a significant impact on the thermal well-being of a person. Meteorological conditions, or microclimate, depend on the thermophysical features of the process, climate, season of the year, heating and ventilation conditions.

Human activity is accompanied by the continuous release of heat into the environment. Its amount depends on the degree of physical stress in certain climatic conditions and ranges from 85 J / s (at rest) to 500 J / s (during hard work). In order for physiological processes in the body to proceed normally, the heat released by the body must be completely removed to the environment. Imbalance in the heat balance can lead to overheating or to overcooling of the body and, as a result, to disability, fatigue, loss of consciousness and heat death.

One of the important integral indicators of the thermal state of the body is the average temperature of the body (internal organs) of the order of 36.5 ° C. It depends on the degree of violation of the heat balance and the level of energy consumption during physical work. When performing work of moderate severity and heavy at high air temperature, body temperature can increase from a few tenths of a degree to 1 ... 2 ° C. The highest temperature of internal organs that a person withstands is +43 ° C, the minimum is +25 ° C. The temperature regime of the skin plays a major role in heat transfer. Its temperature varies within quite considerable limits and under normal conditions the average skin temperature under clothes is 30 ... 34 ° C. Under adverse weather conditions in certain parts of the body, it can drop to 20 ° C, and sometimes even lower.

Normal thermal well-being takes place when the heat release Qtp of a person is completely perceived by the environment Qto, i.e. when there is a heat balance Qtp = Qro. In this case, the temperature of the internal organs remains constant. If the body’s heat production cannot be completely transferred to the environment (Qtp> Qto), the temperature of the internal organs rises and such thermal well-being is characterized by the concept of being hot. Thermal insulation of a person who is at rest (resting sitting or lying down) from the environment will lead to an increase in the temperature of internal organs after 1 h by 1.2 ° C. Thermal insulation of a person performing moderate work will cause a temperature increase by 5 ° C and will come close to the maximum allowable. In the case when the environment perceives more heat than it is reproduced by a person (Qtp <Qto), the body is cooled. Such thermal well-being is characterized by the concept of cold.

Heat exchange between a person and the environment is carried out by convection Qk as a result of washing the body with air, heat conductivity Qt, radiation to the surrounding surfaces Ql and during heat and mass transfer (Qtm = Qp + Qd) during the evaporation of moisture removed to the skin surface by sweat glands Qp and during breathing Qd:

A person's feeling of warmth is most often evaluated on a seven-point scale:
1 - very cold; 2 - cold; 3 - cool; 4 - comfortable; 5 - heat; 6 - hot; 7 - very hot.
The thermal sensations of a person dressed in thin trousers, a long-sleeved shirt and light underwear, performing light work in the room for at least 3 hours in a sitting position, can be determined by the formula

$$B_7 = 0.243t + 0{,}049P - 2.803 \tag{4.3}$$

where 7 is the number of points corresponding to a certain heat perception of the worker; / - indoor air temperature, eC;

P - partial pressure of water vapor in the air, kPa, which is determined by the expression P-PUW / 100;

Pн - partial pressure of saturated water vapor at a specific temperature, kPa: at 10*C Pe= 12,513 kPa, at 20 *C = 23,83 kPa, at 30 °C Pe = - 43,25 kPa;

W - relative humidity, %.

$$B_7 = 0.243 \cdot 25 + 0{,}049 \cdot 33.54 \cdot \frac{45}{100} - 2.803 = 4{,}01$$

At a temperature of 25 ° C and a relative humidity of 45%, the number of points which corresponds to a feeling of comfort.

Thermal radiation in hot shops have a decisive effect on the state of the human body. The greatest penetrating power is possessed by the red rays of the visible spectrum and short infrared rays with a wavelength of up to 1.5 μm, which penetrate deeply into the tissues and are little absorbed by the skin surface. Rays with a wavelength of about 3 microns cause heating of the skin surface.

The permissible intensity of thermal radiation at workplaces from production sources (materials, products, etc.) heated to the glow temperature should not exceed the values specified in table 1.

Table 4.1 - The permissible intensity of thermal radiation

Irradiated body surface, %	The intensity of thermal radiation, W / mg
50 and more	35
From 25 to 50	70
No more 25	100

The permissible intensity of thermal radiation working from radiation sources heated to white and red glow (red-hot or molten metal, glass, flame, etc.) should not exceed 140W / m2. At the same time, more than 25% of the body surface should not be exposed to radiation and the use of personal protective equipment, including face and eye protection, is mandatory.

The intensity of radiation in hot shops is much higher than that tolerated by the body. So, the radiation intensity at workplaces in open-hearth and electric steel-smelting shops reaches 13.9 kW / m2, in converter rooms - 10.4 kW / m2, in domain - 14.6 kW / m2. The irradiation intensity, W / m2, can be approximately determined by the formula:

$$q = 3{,}26 \frac{F}{l^2} [(0.01T)^4 - 110] \qquad (4.4)$$

where F is the area of their buckling surface, m2;

l —Distance from the center of the radiating surface to the irradiated object, m;

G — temperature of the radiating surface. K: on the outer surfaces of 773 K, on the inner - 1473 K, for molten aluminum - 933 K, for molten steel - 1673 ... 1803 K, for flame — 2073 K, for flame of arc furnaces and welding machines — more than 2273 K.

Two heating furnaces are installed in the thermal workshop. Determine the intensity of thermal radiation of the workshop worker if the area of the furnace outer surface radiating towards the worker is F = 14 m2, the furnace surface temperature is T - 338 K, and the distance from the center of the radiating surface to the worker is / = 3.75 m. The irradiated surface of the worker's body is 15 %.

Since / = 3.75 <F = 28, the intensity of thermal exposure of the employee is determined by the formula

$$q = 3{,}26\frac{F}{l^2}[(0.01T)^4 - 110] = 3{,}26\ \frac{\sqrt{28}}{3{,}75}[(0{,}01 \cdot 338)^4 - 110] = 94{,}4\ W/m^2$$

The calculation result shows that the intensity of thermal exposure of the employee does not exceed the permissible value: 100 W / m2.

The intensity of thermal radiation working from open sources (heated metal, glass, open flame, etc.) should not exceed 140 W / m2, while more than 25% of the body surface should not be exposed to radiation and personal protective equipment must be used.

According to GOST 12.1.005–88, optimal and permissible microclimatic conditions can be established in the working area of the production room. Optimal microclimatic conditions are such a combination of microclimate parameters that, with prolonged and systematic exposure to humans, provides a feeling of thermal comfort and creates the prerequisites for high performance. Permissible microclimatic conditions are such combinations of microclimate parameters that, with prolonged and systematic exposure to humans, can cause stress of thermoregulation reactions and which do not go beyond physiological adaptive capabilities. In this case, there are no disturbances in the state of health, there are no uncomfortable heat sensations that worsen well-being and a decrease in working capacity. Optimum microclimate parameters in industrial premises are provided by air conditioning systems, and acceptable parameters are provided by conventional ventilation and heating systems.

5 Technical and Economic Project Justification

5.1 Calculation of capital investments for the implementation of the project

Thesis considers methods of effective design and calculation of exoskeleton structures that regulate human movement.

Modern technologies are firmly embedded in people's lives, and every year their position is becoming stronger. For many people, they have become an integral part of life. To say that this is bad is to consider only one aspect of the process, as new technologies have more advantages than disadvantages.

Wireless networks, communications, complex applications, pulses and other inventions are always made only to make a person feel better, to make his work as easy as possible and to improve his life.

The purpose of the thesis: to increase the strength of human muscles and expand the amplitude of movements due to the outer frame and leading parts.

The exoskeleton replicates human biomechanics to increase the force proportionally during movement.

In the general task of calculation and construction of an exoskeleton we consider the following cases:

- The concept of the exoskeleton;
- determination of exoskeleton calculation and assembly costs;
- calculation of labor intensity and duration of calculation and assembly;
- calculation of salaries of employees who went to the calculation and assembly;
- social transfer account;
- calculation of the cost of materials;
- depreciation charges;
- calculation of the projected cost of work.

To calculate capital investments, we use the formula:

$$K = Kpr + Kob + Ksb + Ktr + Km + Cn \tag{5.1}$$

where Kpr - capital investment in the development of the project, tenge;

Kob - equipment costs, tenge;

Kmon - capital investments for the assembly of a exoskeleton, tenge;

Ktr - capital investments in transport services, tenge;

Km - capital investments for the purchase of materials, tenge;

Cn - capital investments for software development, tenge.

Project development costs are calculated by the formula:

$$Kpr = Zfot + Zc + Zob + Zn \tag{5.2}$$

where CRC - project costs, tenge;

Zfot - general payroll fund for developers, tenge;
Зc - deductions for social tax, tenge;
Zob - special equipment, tenge;
Zn - overhead, tenge.

The total payroll of developers (Zfot) is calculated as the sum of the main and additional wages according to the formula:

$$Zfot = Zo + Zd \tag{5.3}$$

where Zo - the basic salary, tenge;

Zd - additional salary, tenge. The project involves 2 people. Additional salary of employees, which takes into account illness, holidays and other unforeseen circumstances (on average 10% of the basic salary). In order to calculate the basic salary of the contractor.

Project participants and their salaries are presented in table 5.1.

Table 5.1 - Basic salary for system development

No.	The name of the stages	Performers (by category)	Labor input (people / days)	Official salary (tenge)	Cost 1 person (tenge)	Salary (tenge)
1	Pneumatic development	Design engineer	2	186000	6000	12000
2	Programming	Design engineer	2	186000	6000	6000
3	3D model design	Design engineer	1	186000	6000	6000
4	Development of working documentation	Supervisor	1	232500	7500	15000
		Design engineer	1	186000	6000	6000
5	Engineering analysis	Design engineer	2	186000	6000	6000
6	Checking	Supervisor	1	232500	7500	7500
		Total	10			58500

Thus, with the consistent execution of all the stages of work listed in table 1, the total duration of the one-time work will be 10 working days. Additional salary of employees, which takes into account illness, holidays and other unforeseen circumstances (on average 10% of the basic salary):

$$Zd = Zo \times Nd / 100 \tag{5.4}$$

where Nd - the coefficient of additional salaries of developers.

$$Zd = 0.1 \times 58500 = 5850 \text{ (tenge).}$$

According to formula 5.3, the wage fund will be:

$$Zfot = 5850 + 58500 = 64350 \text{ (tenge).}$$

The deductions for the unified social tax are calculated based on the employee's salary and make up 9.5% (Article 358 para. 1 of the Tax Code of the Republic of Kazakhstan):

$$Zc = (Zfot - PO) \times 9.5\% \tag{5.5}$$

where PO is the contribution to the Pension Fund in the Republic of Kazakhstan, which is calculated by the formula:

$$PO = Zfot \times 10\% \tag{5.6}$$

So,

$$PO = 64350 \times 0.1 = 6435 \text{ (tenge).}$$

$$Zc = (64350 - 6435) \times 0.095 = 5501.925 \text{ (tenge).}$$

The cost of special equipment for experimental work is 79500 tenge (table 5.2).

Table 5.2 - Costs of special equipment

No. p / p	Name of materials	Quantity, pcs	Price, tenge	Cost, tenge
1.	A computer	1	70,000	70,000
2.	Soldering kit	1	9500	9500
	Total			79500

Overhead costs make up 30% of the salary:

$$Zn = 0.3 * 64350 = 19305 \text{ (tenge).}$$

Thus, according to formula 2, the cost of developing research will be:

$$KPR = 64350 + 6370.65 + 79500 + 19305 = 163792.65 \text{ (tenge).}$$

Capital investments in equipment amount to 52,300 tenge. The list of necessary equipment is presented in table 5.3.

Table 5.3 - List of equipment necessary for the implementation of the project

Name of equipment	Quantity, units	Price per unit, tg	Cost including VAT, tg	Cost without VAT, tg
Air compressor	1	7500	8400	7500
Carabiner (Mount)	6	1150	7728	6900
Cable braid "Snake skin", m	2	2000	4480	4000
Arduino Kit - "Maker"	1	29000	32480	29000
Pneumatic tube 12x8 mm	2	2450	5488	4900
Total			58576	52300

To calculate the capital investment for the assembly, we use the formula:

$$Ksb = Kob \times 10\% \tag{5.7}$$

Ksb = 54500 × 10% = 10280 (tenge)

Capital investments in transport services are calculated by the formula:

$$Cdr = Cob \times 5\% \tag{5.8}$$

So,

Ktr = 54500 × 5% = 5140 (tenge).

Capital investments in materials necessary for the implementation of the project are presented in table 5.4

Table 5.4 - Material Costs

No.	Name of materials	Quantity, pcs	Price, tenge	Amount, tenge
1.	Solder	1	1500	1500
2.	Rosin	1	100	100
3.	Soldering Acid	1	400	400
4.	Connecting wires	10	10	100

5.	Ethanol	2	200	400
6.	Mount	5	135	675
	Total			3165

Costs (Cn) for software development can be found by the formula:

$$\mathrm{Cn} = \mathrm{Zphot} + \mathrm{Zc} + \mathrm{Pm} + \mathrm{Pe} + \mathrm{Pn} \tag{5.9}$$

where Zfot is the general payroll fund for developers, tenge;

Zc - deductions for social tax, tenge;
Pm - depreciation costs of equipment, tenge;
Re - electricity costs, tenge;
Pn - overhead expenses, tenge.

The size of the payroll fund for developers (PFAT) is calculated according to formula 5.3. In order to calculate the basic salary of the contractor, we use the formula:

$$\mathrm{Zo} = \mathrm{tp} \times \mathrm{Zpo} \tag{5.10}$$

where tp - the complexity of software product development, person-days;

Zpo - daily salary of the developer, (tenge).

Total labor costs are calculated as the sum of the composite labor costs according to the formula:

$$\mathrm{t} = \mathrm{to} + \mathrm{ta} + \mathrm{tb} + \mathrm{tn} + \mathrm{tl} + \mathrm{td} \tag{5.11}$$

Where to is the time spent on the task description, person / hour;

ta - compilation of the program algorithm, person / hour;
tн - time spent writing a program, person / hour;
tb - time to develop a flowchart, person / hour;
totl - time allotted for debugging software on a PC, person / hour;
td - time spent on the development of documentation, person / hour.

The conditional number of operators in the task program is determined by the formula:

$$\mathrm{Q} = \mathrm{q} \times \mathrm{c} \tag{5.12}$$

Where Q is the conditional number of operators;

q is the estimated number of operators depending on the type of task;

c - coefficient taking into account the novelty and complexity of the program.

Let us select the coefficient q according to table 5.5.

Table 5.5 - The values of the coefficient q

Task type	Coefficient of measurement of the coefficient
Accounting tasks	1400 to 1500
Operational management tasks	1500 to 1700
Planning tasks	3000 to 3500
Multivariate tasks	4,500 to 5,000
Complex tasks	5000 to 5500

Since the setting of the pneumatic exoskeleton system is considered in this project, we take the q factor equal to 1400.

Further, in order to determine the coefficient c, the first thing is to choose a group according to the degree of novelty:

- Group A - the development of fundamentally new tasks;
- Group B - development of original programs;
- group G - development of programs using standard solutions;
- Group D - a one-time standard task.

The program will be written in a high-level language using standard algorithms. Now, based on table 4.6, we determine the coefficient c equal to 1.08.

Table 5.6 - Labor calculation factors

Programming language	Difficulty group	Degree of novelty				Coefficient b
		A	B	C	D	
High level	1	1.38	1.26	1.15	0.69	1,2
	2	1.30	1.19	1,08	0.65	1.35
	3	1.20	1.10	1.00	0.60	1,5

Thus, Q = 1400 × 1.08 = 1512 (teams).

After this, it is necessary to determine the time spent on creating the software at each stage:

a) then taken on the fact of:

$$\text{to} = 24 \text{ (person / hour).}$$

b) we find by the formula:

$$\text{ta} = \text{Q} / (50 \times \text{K}) \tag{5.13}$$

where K is a coefficient taking into account the qualifications of a programmer (table 5.7).

Table 5.7 - Programmer qualification factors

Experience	Qualification ratio
Up to 2 years	0.8
2-3 years	1
3-5 years	1.1-1.2

5-7 years old	1.3-1.4
More than 7 years	1.5-1.6

In this way,

$$ta = 1500 / (50 \times 1) = 30 \text{ (person / hour).}$$

c) tH we find by the formula:

$$tH = Q \times 1.5 / (50 \times K) \tag{4.14}$$

Thus, according to formula 5.14:

$$tH = 1500 \times 1.5 / (50 \times 1) = 45 \text{ (person / hour)}$$

d) heat is determined by the formula:

$$t_{otl} = Q \times 4{,}2 / 50 \times K \tag{5.15}$$

According to the formula 5.15:

$$totl = 1500 \times 4.2 / 50 \times 1 = 126 \text{ (person / hour)}$$

d) td, is taken upon the fact and is (from 3 to 5 days for 8 hours):

$$td = 24 \text{ (person / hour).}$$

f) tb is determined similarly to ta by the formula 5.13

Based on the formula 5.11:

$$t = 24 + 30 + 45 + 126 + 24 + 30 = 279 \text{ (hour).}$$

Thus, the time taken to create the software is 279 hours, or 34.875 people/day. The daily wage is determined based on the monthly salary of the developer and the number of working days in the month (on average, 22 working days can be accepted). It is necessary to determine the time spent on creating the software. Information on the employees involved in the development is presented in table 5.8.

Table 5.8 - Information on the employees involved in the project

Specialist - Contractor	Number of persons	Salary per month, tenge
Design engineer	1	126000
Total		126000

The results of the calculation of basic wages are presented in table 5.9.

Table 5.9 - Summary results of the calculation of the costs of the basic wage

Name of the content of work	Executor	Labor input, norm-hour	Salary per hour of work	Salary amount
1	1	8	750	6000

The basic salary is calculated by the formula:

$$Zo = tp \times Zpo \tag{5.16}$$

where tp - the complexity of software product development, person-days;
Zpo - daily salary of the developer, tenge (table 5.9).
In this way,

$$Zo = 34.875 \times 6000 = 209{,}250 \text{ (tenge).}$$

Additional salary (Zd) is calculated by the formula 5.4:

$$Zd = 209{,}250 \times 0.1 = 20{,}925 \text{ (tenge).}$$

Thus, the payroll is:

$$ZFOT = 209250 + 20925 = 230\,175 \text{ (tenge).}$$

Social tax is calculated using the formula 4.5. Where software and another hardware consume wastes is calculated by the formula 5.6.
So,

$$PO = 230175 \times 10\% = 23017.5 \text{ (tenge).}$$

In this way,

$$Zc = (230175 - 23017.5) \times 9.5\% = 19679.96 \text{ (tenge).}$$

Depreciation costs are calculated using the formula:

$$PM = \frac{Собор \times Ha \times N}{100 \times 12 \times t} \tag{5.17}$$

where Na is the depreciation rate (25%);
Cathedral - the initial cost of equipment (tenge);
N - time of use of a personal computer (days);
t is the number of working days in a month.

$$PM = \frac{81200 \times 0{,}25 \times 37{,}4}{100 \times 12 \times 22} = 28.8 \text{ (tenge)}.$$

Electricity costs are calculated by the formula:

$$Re = M \times k \times T \times CkWh \tag{5.18}$$

where M is the power of the computer, kW;

k is the load factor (0.8);

CkWh - the cost of 1 kWh of electricity, tenge / kWh;

T - work time, hour.

In this way,

$$Re = 0.08 \times 0.8 \times 235.71 \times 17.81 = 268.7 \text{ (tenge)}.$$

Overhead costs (Pн) make up 20% of the basic salary:

$$PH = 209250 \times 20\% = 41850 \text{ (tenge)}.$$

Thus, according to formula 5.9, the costs of software development will be:

$$Cn = 230175 + 23017.5 + 28.8 + 268.7 + 41850 = 295340.1 \text{ (tenge)}.$$

Thus, according to formula 5.1, the total amount of capital investment for the project without VAT is equal to:

$$K = 52300 + 5230 + 2615 + 3165 + 163792 + 295340 = 522442 \text{ (tenge)}.$$

5.2 Calculation of the economic efficiency of the project

Evaluation of the economic efficiency of the project is based on the indicator of comparative economic efficiency according to the formula:

$$E = C - K \times E \tag{5.19}$$

where E is the expected annual economic effect, tenge;

C - price when selling the device, tenge,

K - capital investments, tenge;

E - normative coefficient of economic efficiency of capital investments, which is determined by the formula:

$$E = \frac{1}{T_H} \tag{5.20}$$

where Tn is the standard payback period for capital investments, which is 15 years. Thus, according to formula 5.20:

$$E = \frac{1}{15} \approx 0.06$$

The price will be equal to 150,000 tenge.

Based on the expected formula 5.19, the economic effect (E) will be 118,653.43 (tenge). The coefficient of economic efficiency of capital costs is calculated by the formula:

$$Ep = \frac{C}{K} \qquad (5.21)$$

where EP is the coefficient of economic efficiency of capital costs;

C - price when selling the device, tenge;

K - capital investments to create a system, tenge;

E - normative coefficient of economic efficiency of capital investments.

$$Ep = \frac{150000}{522442.75} \times 100\% = 28.7\%.$$

The payback period of capital investments is calculated by the formula:

$$Tr = \frac{1}{E_p} \qquad (5.23)$$

and is:

$$Tr = \frac{1}{0{,}287} = 3.48 \text{ (year)}.$$

The summary results of the calculation of the economic efficiency of the project are presented in table 5.10

Table 5.10 - Indicators of economic efficiency

Indicators	
Capital investments, tenge	522442.75
Expected economic effect, tenge	118,653.43
Coefficient of economic efficiency, %	28.7
Payback period, year	3.48

Conclusion

As a result of the graduation project, skills were obtained in research, in analyzing the operation of an exoskeleton of a knee consisting of artificial muscles working on pneumatic muscles. It will be developed as test models in the field of pneumatic systems. Using these experimental models based on pneumatics, which have intuitive and attractive operating principles, both in theoretical and practical parts, the opportunity to learn about the design of mechanical systems, mathematical descriptions of practical systems, identification of parameters of real processes, modeling non-linear and linearized models systems, consideration of various control methods and their experimental verification. Thus, the use of exoskeleton in the field of medicine will help many patients who have walking problems.

As a result of economic calculation, we can conclude that the payback time of investments in the described exoskeleton is less than years. However, the benefit is designed for the prospect of long-term use.

The analysis of the general microclimate, as well as the calculation of the optimal lighting mode when working on the design of the system, was also carried out. Given what kind of lighting is installed in technical rooms, it is worth noting that the optimal lighting mode of the room calculated by us allows us to double the safety of engineers.

References

1. F. Ferrati, R. Bortoletto, E. Pagello, Virtual modelling of a real exoskeleton constrained to a human musculoskeletal model, in:Living Machines, 2013, pp.96–107.
2. Chang W. H., Kim Y. H. Robot-assisted Therapy in Stroke Rehabilitation // J Stroke. 2013, Sep; 15(3):174-81. doi: 10.5853/jos.2013.15.3.174. Epub 2013 Sep.
3. Chen Y., Li G., Zhu Y., Zhao J., Cai H. Design of a 6-DOF upper limb rehabilitation exoskeleton with parallel actuated joints // Biomed Mater Eng. 2014; 24(6):2527-35. doi: 10.3233/BME-141067.
4. Computer simulation of the hydraulic control system for exoskeleton / Borovin G. K., Kostyuk A. V. G. Seet3 05-7/ 280. — M. 2004. — P. 33.
5. Kazerooni H. Human Augmentation and Exoskeleton Systems in Berkeley // International Journal of Humanoid Research. Vol. 4, N 3, Sep 07.
6. Knaepen K., Beyl P., Duerinck S., Hagman F., Lefeber D., Meeusen R. Human-robot interaction: kinematics and muscle activity inside a powered compliant knee exoskeleton // IEEE Trans Neural Syst Rehabil Eng. 2014. Nov.; 22(6):1128- 37. doi:10.1109/TNSRE.2014.2324153.
7. Klauer C., Schauer T., Reichenfelser W., Karner J., Zwicker S., Gandolla M., Ambrosini E., Ferrante S., Hack M., Jedlitschka A., Duschau-Wicke A., Gfohler M., Pedrocchi A. Feedback control of arm movements using Neuro-Muscular Electrical Stimulation (NMES) combined with a lockable, passive exoskeleton for gravity compensation // Front Neurosci. 2014, Sep 2; 8:262. doi: 10.3389/ fnins.2014.00262.
8. S. D. Rossi, N. M. M. Vitiello, NT. Lenzi, "Sensing pressure distribution on a lower-limb exoskeleton physical human-machine interface", Sensors, vol. 11, no. 1, pp. 207-227, 2010.
9. D. Baiden, and O.Ivlev, "Human-robot-interaction control for orthoses with pneumatic soft-actuators--concept and initial trails", International Conference on Rehabilitation Robotics, pp. 66503536650353, 2013.
10. Z. Xiaobiao, "Design of a Control System for a Lower Limb Exoskeleton Rehabilitation Walking Robot", Shanghai Jiao Tong University, China, 2013.
11. Villegas, D.; van Damme, M.; Vanderborght, B.; Beyl, P.; Lefeber, D. Third-Generation Pleated Pneumatic Artificial Muscles for Robotic Applications: Development and Comparison with McKibben Muscle. Adv. Robot. 2012, 26, 1205–1227.
12. T. P. Dao and S. C. Huang, "An Optimal Study of a Gripper Compliant Mechanism Based on FuzzyTaguchi Method," Applied Mechanics and Materials, vol. 418, pp. 141-144, 2013.

13. S.-C. Huang and T.-P. Dao, "Design and computational optimization of a flexure-based XY positioning platform using FEA-based response surface methodology," International Journal of Precision Engineering and Manufacturing, vol. 17, pp. 1035-1048, 2016.

14. K. P. Tee; E. Burdet, C. M. Chew, T. E. Milner, "A model of force and impedance in human arm movements" Biol. Cybern, vol. 90, pp. 368–375, 2004.

15. L. E. Miller, A. K. Zimmermann, and W. G. Herbert, “Clinical effectiveness and safety of powered exoskeleton-assisted walking in patients with spinal cord injury: systematic review with metaanalysis,” Med. Devices Auckl. NZ, vol. 9, pp. 455–466, 2016.

16. A. J. Young and D. P. Ferris, “State of the Art and Future Directions for Lower Limb Robotic Exoskeletons,” IEEE Trans. Neural Syst. Rehabil. Eng., vol. 25, no. 2, pp. 171–182, Feb. 2017.

17. U. Onen, F.M. Botsali, M. Kalyoncu, M. Tinkir, N. Yilmaz, Y. Sahin, Design and actuator selection of a lower extremity exoskeleton, IEEE/ASME Trans. Mechatronics 19 (2014) 623–632.

18. R.J. Farris, H.a. Quintero, M. Goldfarb, Preliminary evaluation of a powered lower limb orthosis to aid walking in paraplegic individuals, IEEE Trans. Neural Syst. Rehabil. Eng. 19 (2011) 652–659.

19. Wu T. M., Chen D. Z. Biomechanical study of upper-limb exoskeleton for resistance training with three-dimensional motion analysis system // J Rehabil Res Dev. 2014; 51(1):111-26. doi: 10.1682/ JRRD.2012.12.0227.

20. Yong-Lae Park / Design and control of a bio-inspired soft wearable robotic device for ankle, foot rehabilitation // Bioinspir. Biomim. 2014, 9 —P. 45—51.

21. Yu H., Huang S., Thakor N. V., Chen G., Toh S. L., Sta Cruz M., Ghorbel Y., Zhu C. A novel compact compliant actuator design for rehabilitation robots // IEEE Int Conf Rehabil Robot. 2013, Jun; 2013:6650478. doi:10.1109/ ICORR.2013.6650478.

22. Kao, P. C., Lewis, C. L., and Ferris, D. P.: Invariant ankle moment patterns when walking with and without a robotic ankle exoskeleton, J. Biomech., 43, 203–209, 2010.

23. Lajeunesse, V., Vincent, C., Routhier, F., Careau, E., and Michaud F.: Exoskeletons’ design and usefulness evidence according to a systematic review of lower limb exoskeletons used for functional mobility by people with spinal cord injury, Disabil. Rehabil. Assist. Technol., 11, 535–547, https://doi.org/10.3109/17483107.2015, 2016.

24. Li, T., and Ceccarelli, M.: Design and simulated characteristic sofa new biped mechanism, Robotica, 33, 1568–1588, 2015.

25. Young Aaron, J. and Ferris, D. P.: State-of-the-art and Future Directions for Lower Limb Robotic Exoskeletons, IEEE Trans. Neural. Syst. Rehabil. Eng., 171–182, https://doi.org/10.1109/TNSRE.2016.2521160, 2017